

**APPLICATION OF COMPOSITE PDMS/PVDF
MEMBRANE IN PERSTRACTION SYSTEM OF
ETHANOL FERMENTATION IN FED-BATCH PROCESS
FROM CANE MOLASSES**

Pailin Panvichit

A Thesis Submitted in Partial Fulfillment of the Requirements for the

Degree of Master of Science in Biotechnology

Suranaree University of Technology

Academic Year 2005

ISBN 974-533-522-3

การประยุกต์ใช้เยื่อแผ่นเชิงประกอบชนิด PDMS/PVDF กับ
ระบบเพอร์สแทรกชั้นในกระบวนการผลิตเอทานอลในการหมักแบบกึ่งกะ
จากกากน้ำตาลอ้อย

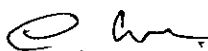
นางสาวไพลิน แพนวิจิต

วิทยานิพนธ์นี้เป็นส่วนหนึ่งของการศึกษาตามหลักสูตรปริญญาวิทยาศาสตรมหาบัณฑิต
สาขาวิชาเทคโนโลยีชีวภาพ
มหาวิทยาลัยเทคโนโลยีสุรนารี
ปีการศึกษา 2548
ISBN 974-533-522-3

**APPLICATION OF COMPOSITE PDMS/PVDF MEMBRANE IN
PERSTRATION SYSTEM OF ETHANOL FERMENTATION IN
FED-BATCH PROCESS FROM CANE MOLASSES**

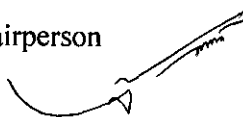
Suranaree University of Technology has approved this thesis submitted in partial fulfillment of the requirements for a Master's Degree.

Thesis Examining Committee



(Asst. Prof. Dr. Chokchai Wanapu)

Chairperson



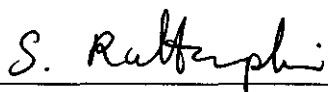
(Dr. Apichat Boontawan)

Member (Thesis Advisor)



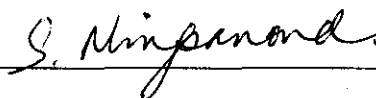
(Asst. Prof. Dr. Sunthorn Kanchanatawee)

Member



(Assoc. Prof. Dr. Saowanee Rattanaphani)

Vice Rector for Academic Affairs



(Asst. Prof. Dr. Suwayd Ningsanond)

Dean of Institute of Agricultural Technology

โพลิน แผนวิจิต : การประยุกต์ใช้เยื่อแผ่นแข็งประกอบชนิด PDMS/PVDF กับระบบเพอร์สแทรกชัน
ในกระบวนการผลิตเอทานอลในการหมักแบบกึ่งกะจากกากน้ำตาลอ้อย (APPLICATION OF
COMPOSITE PDMS/PVDF MEMBRANE IN PERSTRATION SYSTEM OF
ETHANOL FERMENTATION IN FED-BATCH PROCESS FROM CANE
MOLASSES) อาจารย์ที่ปรึกษา : ดร.อภิชาติ บุญทาวน, 101 หน้า. ISBN 974-533-522-3

กระบวนการหมักเอทานอลจะสิ้นสุดลงจากปฏิกิริยาการยับยั้งการเจริญของเชื้อยีสต์ เนื่องจากปริมาณเอทานอลที่สะสมในน้ำหมัก จะทำให้การหมักสิ้นสุดลง ปัญหานี้ ทำให้ผลผลิตที่ได้ (yield) มีค่าต่ำ ส่งผลให้ต้นทุนการผลิตสูง ด้วยเหตุนี้จึงได้มีการประยุกต์ใช้เยื่อแผ่นซิลิโคนในถังปฏิกรณ์ชีวภาพร่วมกับ การสกัดโดยใช้ตัวทำละลายอินทรีย์ หรือที่เรียกว่า ระบบเพอร์สแทรกชัน (Perstraction) ซึ่งเทคนิคดังกล่าว จะใช้เยื่อแผ่นยางซิลิโคนชนิด Polydimethylsiloxane (PDMS) ที่มีความหนาประมาณ 2-5 ไมโครเมตร ซึ่งมีลักษณะเป็นแผ่นใส และไม่มีรูพรุน (dense polymeric material) โดยเคลือบบนเยื่อแผ่นรองรับ (supporting layer) พอลิเมอร์ชนิด polyvinylidene fluoride (PVDF) ซึ่งเมื่อส่องด้วยกล้องจุลทรรศน์อิเล็กตรอนแบบส่องกราด พบว่ามีลักษณะคล้ายนิ้วมือ อีกทั้งเยื่อแผ่น PVDF มีความแข็งแรง และมีลักษณะความเป็นรูพรุนสูง เป็นตัวกั้นน้ำหมักกับตัวทำละลายอินทรีย์ออกจากกัน ซึ่งยางซิลิโคนจะมีคุณสมบัติไม่ชอบน้ำ (hydrophobic property) จากการทดลอง เมื่อทำการแปรผันค่า Reynolds number ในด้านของผสมน้ำ-เอทานอล พบว่าค่าสัมประสิทธิ์การถ่ายเทมวลทั้งหมด (k_{ov}) มีค่าอยู่ระหว่าง 3.0×10^{-7} – 4.21×10^{-6} เมตรต่อวินาที โดยค่านี้จะขึ้นอยู่กับค่า Reynolds number และความหนาของเยื่อแผ่น และจากการศึกษาความเข้มข้นของเซลล์เริ่มต้นในกระบวนการหมัก พบว่า เซลล์ที่ความเข้มข้นสูง จะมีการผลิต เอทานอลได้สูง ดังนั้นงานวิจัยนี้ทำการเลี้ยงเซลล์ให้ได้ชีวมวลความเข้มข้นสูงมากกว่า 25 กรัมต่อลิตรในสูตรอาหารเฉพาะ (ความเข้มข้น 3 เท่า ของสูตรอาหาร YM) เพื่อที่จะเพิ่มอัตราการผลิต อีกทั้งลดความเป็นพิษต่อเซลล์ที่เกิดจากสารตั้งต้นและผลิตภัณฑ์ และใช้ความเข้มข้นของเซลล์สูงนี้ เป็นหัวเชื้อในกระบวนการหมักแบบกึ่งกะ ซึ่งมีอัตราการป้อนของกากน้ำตาลอ้อยที่ต่างกัน เพื่อเปรียบเทียบอัตราการผลิตเอทานอลของแต่ละอัตราการป้อน ผลการทดลองพบว่าที่อัตราการป้อน 0.006 กรัมต่อวินาทีต่อกรัมเซลล์ มีความสามารถในการผลิตเอทานอลสูงสุด คือ 4.83 กรัมต่อลิตรต่อชั่วโมง และความเข้มข้นเอทานอลสูงสุด คือ 171 กรัมต่อลิตร

การศึกษการถ่ายเทมวลร่วมกับจลนศาสตร์การหมัก สามารถที่จะคำนวณหาพื้นที่ผิวของเยื่อแผ่นที่ต้องการจากอัตราการผลิตเอทานอลโดยเชื้อยีสต์ ในกระบวนการหมัก พบว่าพื้นที่ผิวเยื่อแผ่นที่เหมาะสม สำหรับกระบวนการนี้มีค่าประมาณ 50 ตารางเซนติเมตร โดยมีค่าปริมาตรเริ่มต้นของน้ำหมักเท่ากับ 1 ลิตร จากนั้นทำการหมักเอทานอลแบบกึ่งต่อเนื่อง พร้อมทั้งใช้เทคนิคเพอร์สแทรกชันซึ่งใช้เยื่อแผ่น พร้อมทั้งตัวทำละลายอินทรีย์ เป็นตัวช่วยเก็บเกี่ยวเอทานอลออกจากถังหมัก พบว่า ผลผลิตและความสามารถในการผลิตเอทานอล จะสูงกว่า กระบวนการหมักแบบกึ่งกะ (12.0 กรัม_{เอทานอล}ต่อกรัม_{เซลล์} เทียบกับ 9.8 กรัม_{เอทานอล}ต่อกรัม_{เซลล์}) และได้ความเข้มข้นของเอทานอลสูงสุด เท่ากับ 300 กรัมต่อลิตร

อีกทั้ง กระบวนการนี้เมื่อทำการวัดเซลล์ได้กึ่งจูลทรศน์อิเล็กตรอน พบว่า สามารถลดอัตราการตายของเซลล์ได้จาก 2.47×10^{-2} ต่อชั่วโมง ในกระบวนการหมักแบบกึ่งกะ เป็น 1.50×10^{-2} ต่อชั่วโมง แต่อย่างไรก็ตาม ผลผลิตของเอทานอลที่ได้ยังต่ำกว่าที่คาดหวังไว้ อาจเนื่องจากการยับยั้งของผลผลิตที่เชื้อจุลินทรีย์สร้างขึ้น

สาขาวิชาเทคโนโลยีชีวภาพ
ปีการศึกษา 2548

ลายมือชื่อนักศึกษา ไพรัตน์ พงษ์วัฒน์
ลายมือชื่ออาจารย์ที่ปรึกษา [ลายมือ]
ลายมือชื่ออาจารย์ที่ปรึกษาร่วม [ลายมือ]

PAILIN PANVICHIT : APPLICATION OF COMPOSITE PDMS/PVDF
MEMBRANE IN PERSTATION SYSTEM OF ETHANOL FERMENTATION
IN FED-BATCH PROCESS FROM CANE MOLASSES. THESIS ADVISOR :
APICHAT BOONTAWAN, Ph.D. 101 PP. ISBN 974-533-522-3

YEAST, ETHANOL FERMENTATION, COMPOSITE PDMS/PVDF MEMBRANE, A
PERSTATION SYSTEM

In ethanol fermentation, product inhibition is a major problem affecting both yield and volumetric productivity. This work employed a conventional stirred-tank bioreactor equipped with an external flat sheet composite membrane unit to separate ethanol from fermentation broth into 1-decanol as an organic solvent. The membrane was fabricated in our laboratory and was comprised of a thin non-porous polydimethyl siloxane (PDMS) selective layer coated on a microporous support layer cast from polyvinylidene fluoride (PVDF). Characterizations of the membranes were carried out using SEM, and revealed a thin film of PDMS with a thickness of approximately 2-5 μm coated on a finger-like structure of the PVDF support layer. The overall mass transfer coefficients (k_{ov}) were found to be in the range of $3.0 \times 10^{-7} - 4.21 \times 10^{-6} \text{ m.s}^{-1}$ depending mainly on the aqueous hydrodynamic conditions, and thickness of selective layer. High-cell-density cultivation was carried out using special formulated media, and obtained biomass concentration up to 25 g.L^{-1} .

The main objectives of this study were to increase production rate in parallel with reduction of deleterious effects of substrate and/or product inhibition. Fermentation kinetics studies were subsequently investigated in fed-batch process with different feeding rates of molasses. The experimental data showed that feeding rate of $0.006 \text{ g.s}^{-1}.\text{g}^{-1}_{\text{cell}}$

resulted in the estimated membrane area of approximately 50 cm² based on 1 litre of initial working volume. Application of the composite membrane to fed-batch fermentation was then investigated in order to increase the production yields and volumetric productivity. Production yield ($Y_{P/X}$) in the membrane bioreactor was an order of magnitude higher than fed-batch fermentation (12.0 versus 9.80 g_{ethanol}·g⁻¹_{cell}), and resulted in the maximum ethanol concentration of 300 g.L⁻¹. Finally, relative viability of the cell was observed under microscope, and showed a decrease in deactivation constant (k_d) of 1.50×10^{-2} hr⁻¹ compared to 2.47×10^{-2} hr⁻¹ in fed-batch process. However, the yield was lower than expected result. The course of this phenomenon was unclear, but could possibly due to the effect of intermediate product inhibition.

School of Biotechnology

Academic Year 2005

Student's Signature Pailin Panvichit

Advisor's Signature [Signature]

Co-advisor's Signature [Signature]

ACKNOWLEDGEMENT

The research work of this thesis was carried out at Biotechnology laboratory of Suranaree University of Technology. I would like to express a great thankfulness to my advisor, Dr. Apichat Boontawan and my co-advisor, Asst. Prof. Dr. Sunthorn Kanchanatawee, for his infinite encouragement, support, and guidance of my work. Without these things, I could not gain understanding of my research.

I want to thank Arkema (Thailand) for PVDF(Kynar[®] 760). PDMS was kindly provided by Dow corning (Thailand) and Rhodia (Thailand).

I wish to thanks all my friends at school of biotechnology. It has been a real pleasure to work with them, and I appreciate their help.

Finally, I would like to thank all my family for their affection, love, and encouragement. This work could not be achieved without your support.

Pailin Panvichit

CONTENTS

	Page
ABSTRACT IN THAI	I
ABSTRACT IN ENGLISH.....	III
ACKNOWLEDGEMENT.....	V
CONTENTS	
LIST OF FIGURES.....	XI
LIST OF TABLES	XV
LIST OF ABBREVIATIONS	XVI
CHAPTER	
I INTRODUCTION	
1.1 Ethanol Fermentation from molasses	1
1.2 Ethanol fermentation processes.....	5
1.2.1 Batch fermentation.....	5
1.2.2 Continuous fermentation.....	5
1.2.3 Fed-batch fermentation	6
1.3 Technical problems for the production of high purity ethanol.....	9
1.3.1 Problems from biocatalyst	9
1.3.2 Purification problems.....	10
1.4 Extractive Fermentation	11

CONTENT (Continued)

Page

1.5 Membrane separation processes	13
1.5.1 Transport mechanism of hydrophobic solutes through silicone rubber membrane in a liquid-liquid contacting system.....	15
1.6 Composite PDMS/PVDF membrane.....	22
1.7 Membrane bioreactor for continuous separation of organic solutes from the fermentation broth	25
1.8 Thesis Objectives.....	26
1.9 Scope and limitation of the study	27
1.10 Expected results.....	27

CHAPTER

II MATERIALS AND METHODS

2.1 Chemicals	28
2.2 Membrane preparation and characterization.....	28
2.2.1 Preparation of PDMS, and composite PDMS/PVDF membrane	28
2.2.2 Membrane/aqueous partition coefficient, P_{aq}^{mem}	29
2.2.3 Organic/aqueous partition coefficient, P_{aq}^{org}	30
2.2.4 Absorption and diffusivity of ethanol in PDMS	31
2.3 Experimental setup and mass transfer study	31
2.3.1 Membrane module.....	31
2.3.2 Transport mechanism of ethanol through PDMS membrane.....	33

CONTENT (Continued)

	Page
2.4 Fermentation of ethanol from molasses.....	35
2.4.1 Batch culture.....	35
2.4.2 Culture condition for the microorganisms in order to achieve high cell concentration in batch culture.....	36
2.4.3 Fed-batch fermentation.....	36
2.5 Membrane bioreactor setup for <i>in situ</i> ethanol removal in fed-batch fermentation.....	37
2.6 Analysis.....	38
2.6.1 Quantitative analysis of ethanol.....	38
2.6.2 Biomass concentrations.....	39
2.6.3 Sugar concentrations.....	39
2.6.4 Microscopy.....	40
 CHAPTER	
III RESULTS AND DISCUSSIONS	
3.1 Membrane Characterization.....	41
3.1.1 Preparation of PDMS and composite PDMS/PVDF membrane.....	41
3.2 Partition coefficients.....	44
3.2.1 Membrane/aqueous coefficient (P_{aq}^{mem}).....	44
3.2.2 Organic/aqueous partition coefficients (P_{aq}^{org}).....	45
3.3 Mass transfer consideration of a membrane in liquid-liquid contacting system.....	47

CONTENT (Continued)

	Page
3.3.1 Absorption and diffusivity of ethanol in PDMS membrane.....	47
3.3.2 Mass transfer analysis and overall mass transfer coefficient (k_{ov}).....	50
3.3.3 Effect of membrane thicknesses.....	53
3.3.4 Effect of aqueous Reynolds numbers (Re_{aq}).....	55
3.4 Fermentation kinetics.....	57
3.4.1 Effect of initial cell concentrations.....	57
3.4.2 High cell density cultivation.....	59
3.4.3 Effect of molasses feeding rate	61
3.5 Membrane bioreactor setup for <i>in situ</i> ethanol removal in fed-batch fermentation.....	64
3.5.1 Operation of membrane bioreactor for <i>in situ</i> ethanol removal in fed-batch fermentation system.....	66
3.5.2 Investigation for the system stability.....	68
 CHAPTER	
IV CONCLUSIONS AND RECOMMENDATIONS	
4.1 Further Research Works.....	74.
4.1.1 Pretreatment of molasses or usage of more suitable carbon source...76	
4.1.2 Improve the design of membrane module.....	77
4.1.3 Protection against ethanol toxicity.....	79

CONTENT (Continued)

	Page
REFERENCES.....	80
APPENDICES.....	89
APPENDIX A Medium preparation.....	90
APPENDIX B Standard calibration curve.....	91
APPENDIX C Time course of glucose concentrations at molasses feeding rate.....	95
APPENDIX B Time course of glucose concentration at initial cell concentrations.....	98
APPENDIX B Ethanol analysis by gas chromatography.....	101
BIOGRAPHY.....	103

LIST OF FIGURES

Figure	Page
Figure 1 Embden-Meyerhof pathway (Bailey and Ollis, 1986).....	4
Figure 2 Absorption of organic molecules in the membrane matrix.....	16
Figure 3 Concentration profile of organic solute in a hydrophobic membrane organic-aqueous two phase system (Boontawan, 2005).	19
Figure 4 Chemical structure of polydimethylsiloxane polymer (PDMS).....	23
Figure 5 Chemical structure of polyvinylidene fluoride (PVDF).....	23
Figure 6 Schematic diagram of PDMS/PVDF composite membrane casting from dry-wet phase inversion technique showing the dense top layer and finger-liked void structure at the bottom.	24
Figure 7 Schematic diagram for the working principle of perstractive membrane bioreactor (Boontawan, 2005).	26
Figure 8 Schematic diagram of the perstraction membrane module used in this study	32
Figure 9 An experimental set up for separation of ethanol from diluted aqueous solution	33
Figure 10 Membrane bioreactor set up for fed-batch fermentation of ethanol by perstraction technique. A is the molasses, B is the organic solvent, C is the membrane module, and D is the bioreactor.....	38
Figure 11 Scanning electron micrograph of PDMS membrane prepared by solution casting technique.	42

LIST OF FIGURES (Continued)

Figure	Page
<p>Figure 12 SEM picture of composite PDMS/PVDF support membrane casting from phase inversion technique (showed PVDF layer has finger-liked)</p>	43
<p>Figure 13 Scanning electron microscope picture of composite PDMS/PVDF membrane</p>	43
<p>Figure 14 Equilibrium curve of ethanol partitioning into membrane immersed in pentanol, and 1-decanol at 30°C.....</p>	45
<p>Figure 15 Absorption characteristic of ethanol in the PDMS membrane sheet, thickness 100 μm (saturated with 1-decanol) as a function time (T=30°C)</p>	49
<p>Figure 16 Absorption characteristic of ethanol in the PDMS membrane sheet, thickness 100 μm as a function of time (T=30°C)</p>	49
<p>Figure 17 Time course of ethanol concentration in organic reservoir (1-decanol) during the mass transfer experiment using PDMS membrane. ($\delta = 500 \mu\text{m}$, $V_{\text{org}} = 500 \text{ mL}$, $V_{\text{aq}} = 2\text{L}$, initial ethanol concentration in aqueous phase = 10%, 30 °C)</p>	51
<p>Figure 18 Graphical determination of k_{ov} for Figure 17.....</p>	52
<p>Figure 19 Effect of membrane thickness on the k_{ov} ($V_{\text{org}} = 500 \text{ mL}$, $V_{\text{aq}} = 2\text{L}$, $E^0 = 10\%$, $Re_{\text{aq}} = 4000$, $Re_{\text{org}} = 150$, 30 °C).</p>	54
<p>Figure 20 Effect of aqueous phase Re on k_{ov} for the extraction of ethanol from aqueous phase to 1-decanol. ($Re_{\text{org}} = 250$, composite membrane).....</p>	56

LIST OF FIGURES (Continued)

Figure	Page
Figure 21 Time course concentration of ethanol with different initial cell concentrations. (Initial total sugar concentration 125 g.L^{-1} , $T = 30 \text{ }^\circ\text{C}$ and 250 rpm).	57
Figure 22 Effect of biomass concentration on the volumetric productivity (Initial total sugar concentration 125 g.L^{-1} , $T = 30 \text{ }^\circ\text{C}$ and 250 rpm).....	59
Figure 23 High biomass cultivation of <i>S. cerevisiae</i> in 3X YM medium ($\text{pH} = 5.5$, $T = 30 \text{ }^\circ\text{C}$).	61
Figure 24 Effect of feeding rates on performances of molasses fermentation by <i>S. cerevisiae</i> in fed-batch process ($T = 30 \text{ }^\circ\text{C}$, $\text{pH} = 5.5$, $V_0 = 0.75 \text{ L}$).	63
Figure 25 Effect of molasses feeding rate on the volumetric productivity.	64
Figure 26 Organic phase and aqueous phase (bioreactor) concentration of ethanol during fed-batch fermentation in a membrane bioreactor.	67
Figure 27 Deactivation constant study in batch fermentation ($T = 30 \text{ }^\circ\text{C}$, $\text{pH} = 5.5$, biomass concentration = 25 g.L^{-1}).	70
Figure 28 Deactivation constant in fed-batch fermentation (Molasses feeding rate = 0.006 g.s^{-1} , $T = 30 \text{ }^\circ\text{C}$, $\text{pH} = 5.5$, agitation speed = 250 rpm).	71
Figure 29 Deactivation constant of <i>S. cerevisiae</i> in fed-batch fermentation with <i>in situ</i> ethanol removal in a membrane bioreactor.	72
Figure 30 Schematic diagram of the plate-and-frame mass exchanger.	77

LIST OF FIGURES (Continued)

Figure	Page
Figure 31 An experimental setup for a flat sheet membrane bioreactor for <i>in situ</i> removal of ethanol from fermentation broth, A is the membrane module..	78
Figure 32 Standard calibration curve of ethanol using pentanol as organic solvent ..	91
Figure 33 Standard calibration curve of ethanol using decanol as organic solvent ...	92
Figure 34 Standard calibration curve of cell concentration.....	93
Figure 35 Standard calibration curve of sugar concentration.....	94
Figure 36 Time course glucose concentration at molasses feeding rate 0.004, 0.006, 0.01 and 0.02 g.s ⁻¹	95
Figure 37 Time course glucose concentration at initial cell concentration 5, 10, 15, 20 and 25 g.L ⁻¹	96
Figure 38 Chromatogram of ethanol and decanol in ethanol extraction from fermentation broths by using perstraction system.....	97

LIST OF TABLES

Table	Page
Table 1 Important chemical composition of sugar cane molasses (Jaisana <i>et al.</i> , 2000) ..	1
Table 2 Physio-chemical properties of ethanol (Najafpour and Lim, 2002)	3
Table 3 Physio-chemical properties of the organic solvents used in this study.....	30
Table 4 Determination for organic/aqueous partition coefficient of ethanol at 30 °C.....	46
Table 5 Determination for membrane /aqueous partition coefficient and organic/aqueous partition coefficient of ethanol at 30°C.....	47

LIST OF ABBREVIATIONS

A	Membrane area	m^2
C_0	Initial concentration of solute in the aqueous phase	$g.L^{-1}$
C_{aq}	Solute concentration in aqueous phase	$g.L^{-1}$
C_{aq}^i	Interface solute concentration at aqueous side	$g.L^{-1}$
C_{aq}^0	Initial solute concentration in aqueous phase	$g.L^{-1}$
C_{mem}	Equilibrium concentration of solute	$g.L^{-1}$
C_{org}	Solute concentration in organic phase	$g.L^{-1}$
C_{org}^i	Interface solute concentration at organic phase	$g.L^{-1}$
C_x	Cell concentration	$g.L^{-1}$
D	Dilution rate	hr^{-1}
D_i	Diffusivity of the component i	$m^2.s^{-1}$
D_{mem}	Membrane diffusivity	$m^2.s^{-1}$
d^{HR}	Hydraulic diameter	m
E_f	Final concentration of ethanol	$g.L^{-1}$
E^0	Initial concentration of ethanol	$g.L^{-1}$
F	Feed flow rate	$L.hr^{-1}$
F_0	Starting feed flow rate	$L.hr^{-1}$
J_i	Mass flux of component i	$kg.m^{-2}.hr^{-1}$

LIST OF ABBREVIATIONS (Continued)

J_{aq}^i	Mass flux of component i through aqueous boundary layer	$\text{kg.m}^{-2}.\text{hr}^{-1}$
J_{mem}^i	Mass flux of component i through membrane phase	$\text{kg.m}^{-2}.\text{hr}^{-1}$
J_{org}^i	Mass flux of component i through organic boundary layer	$\text{kg.m}^{-2}.\text{hr}^{-1}$
k_{ov}	Overall mass transfer coefficient	m.s^{-1}
k_{aq}	Mass transfer resistance in aqueous phase	m.s^{-1}
k_{mem}	Mass transfer resistance in membrane phase	m.s^{-1}
k_{org}	Mass transfer resistance in organic phase	m.s^{-1}
K_S	Michaelis-Menten constant	g.L^{-1}
M_t	Mass of solute absorbed in the membrane at time = t	g
M_∞	Mass of solute absorbed in the membrane at equilibrium	g
N_i	Mass transfer rate of component i	kg.hr^{-1}
P	Product concentration	g.L^{-1}
p_{aq}^{mem}	Membrane/aqueous partition coefficient	-
p_{org}^{mem}	Membrane/organic partition coefficient	-
p_{aq}^{org}	Organic/aqueous partition coefficient	-
r_E	Average productivity of ethanol	$\text{g.L}^{-1}.\text{hr}^{-1}$
r_S	Substrate consumption rate	$\text{g.L}^{-1}.\text{hr}^{-1}$
r_X	Average productivity of biomass	$\text{g.L}^{-1}.\text{hr}^{-1}$

LIST OF ABBREVIATIONS (Continued)

S	Substrate concentration	g.L^{-1}
S_0	Initial substrate concentration	g.L^{-1}
t	Time	s
t_f	Final time of fed-batch process	s
u	Bulk fluid velocity	m.s^{-1}
V_{aq}	Volume of the aqueous phase	m^3
V_f	Final volume of the fermentation broth	m^3
V_0	Initial volume of the fermentation broth	m^3
V_{org}	Volume of the organic phase	m^3
V_{mem}	Membrane volume	m^3
X	Biomass concentration	g.L^{-1}
X_0	Initial biomass concentration	g.L^{-1}
X_f	Final biomass concentration	g.L^{-1}
	Greek letters	
α	Separation factor or membrane selectivity	-
δ	Membrane thickness	m
ρ	Bulk fluid density	kg.m^{-3}
χ	Chemical potential	-
μ	Bulk fluid viscosity	Pa.s
μ	Specific growth rate	hr^{-1}
μ_{max}	Maximum specific growth rate	hr^{-1}

CHAPTER I

INTRODUCTION

1.1 Ethanol Fermentation from molasses

Molasses, a by-product of sugar manufacturing processes contained approximately 50% (w/w) of total sugars, is mostly used as an animal feed. The quality of molasses depends on the maturity of the sugar cane or beet, the amount of sugar extracted, and the method of extraction. The lowest grade, called blackstrap, is mainly used to mix with cattle feed, and also used in the manufacture of industrial alcohol (Wee, 2004). Molasses has an additional advantage as it is a relatively cheap material, readily available, and is already used for industrial ethanol production (Mubeccel and Mutlu, 1999). The important chemical compositions of molasses are shown in Table 1.

Table 1 Important chemical composition of sugar cane molasses (Jaisana *et al.*, 2000)

Composition	Value (%w/w)
Water	20.65
Sucrose	36.60
Reducing sugar	13.00
Gum and starch	3.01
Ash	15.10
Nitrogen	0.95

Table 1 (Continued) Important chemical composition of sugar cane molasses (Jaisana *et al.*, 2000)

Composition	Value (%)
SO ₂	0.46
P ₂ O ₅	0.12
K ₂ O	4.19
CaO	1.35
MgO	1.12

Ethanol is a clear, colorless liquid with a characteristic, agreeable odor. It has been made since ancient time by the fermentation of sugar in order to produce all sorts of alcoholic beverage. Nowadays, more than half of industrial ethanol is still produced using this conventional process (Nielsen and Villadsen, 2003). More importantly, ethanol is also employed in gasoline formulations for octane enhancement and, increasingly, is used as oxygenate for the control of automotive tailpipe emissions. In addition, ethanol is used in alcoholic beverages and for industrial purpose. It is an alternative fuel blended with gasoline. Ethanol is most commonly used to increase octane and improve the emissions quality of gasoline. In some areas, ethanol is blended with gasoline to form an E10 blend (10% ethanol and 90% gasoline) but it can be used in higher concentration such as E85 or E95. Historically, due to high feedstock prices and competition from other products for its gasoline uses, the economics of the production of this renewable fuel have been marginal for many manufacturing facilities. Improvements of the fuel ethanol production process resulting in even 2-5 cents per gallon could significantly increase its demand. From a technical viewpoint, one approach to process improvement would be the

conversion of the traditional batch to one based upon a truly continuous fermentation (O'Brien *et al.*, 1999). Table shows physio-chemical properties of pure ethanol.

Table 2 Physio-chemical properties of ethanol (Najafpour and Lim, 2002)

Properties	Value
Empirical formula	CH ₃ CH ₂ OH
Molecular weight	46
Normal boiling point, °C	78.32
Critical temperature, °C	243.1
Density, d ₄ ²⁰ , g/ml	0.7893
Heat of combustion at 25°C, J/g	29676.69
Autoignition temperature, °C	793.0

Simple sugars are the raw material for an enzyme from yeast, which changes the sugars into ethanol and carbon dioxide (CO₂). The micro-organisms of primary interest to industrial operations in the fermentation of ethanol include *Saccharomyces cerevisiae*, and *Kluyveromyces sp.* Especially, *S. cerevisiae*, the budding yeast, is the common yeast to be used as either baker's or brewer's yeast.

Alcohol fermentation is the formation of alcohol from sugar. Yeast, when under anaerobic conditions, convert glucose to pyruvic acid via the glycolysis pathways. Fermentation allows the yeast to continue the production of energy and survive in the absence of oxygen, producing ethanol and carbon dioxide from pyruvate. Moreover, glycolysis serves as the only net producer of ATP from the whole process (Hofmeyr, 1997). The step of glycolysis pathway starts from adding two phosphate groups from ATP, then splitting into two 3-carbon molecules as glyceraldehyde-3-phosphate before it

is subsequently oxidized. Since one molecule of glucose produces two 3-C molecules, total yield at this stage is 4 ATPs. The resulting 3-C molecule is pyruvate (Voet, 1995). When oxygen is available, the pyruvate can be converted to acetyl-CoA and enter the Krebs cycle, where the acetyl-CoA will be completely oxidized and generate ATP through oxidative phosphorylation. However, fermentation is much less efficient than oxidative phosphorylation in making ATP, creating only 2 ATP whilst oxidative phosphorylation creates 36 ATP per one molecule of glucose. In conclusion, oxidative phosphorylation does not occur in the absence of oxygen, and yeast gains ATP under anaerobic condition via glycolysis of glucose only. Figure 1 shows the Embden-Meyerhof pathway of ethanol production from glucose.

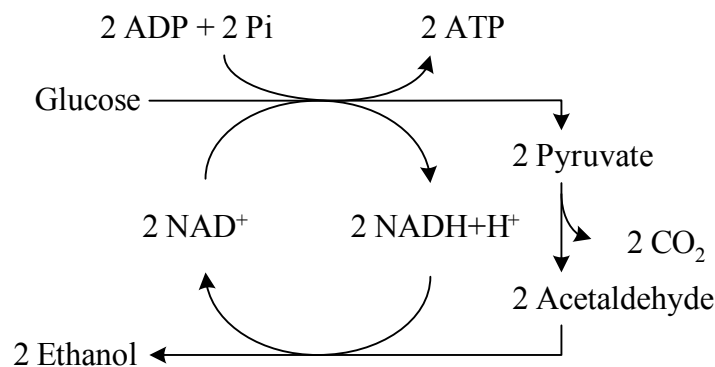


Figure 1 Embden-Meyerhof pathway (Bailey and Ollis, 1986).
1.2 Ethanol fermentation processes

Ethanol fermentation can be divided into 3 processes: batch, continuous, and fed-batch process.

1.2.1 Batch fermentation

During batch fermentation, ethanol accumulates in the surrounding broth. Several studies have been developed that the removal of this accumulated ethanol does not immediately restore fermentative activity, and they provide evidence that the decline in metabolic rate is due to physiological changes (including possible ethanol damage) rather than to the presence of ethanol. During fermentation, ethanol typically accumulates below 12% (v/v). By batch fermentation, using cane molasses were obtained ethanol productivity from 1.73 g.L⁻¹.hr⁻¹ at 37°C (Neelam and Amarjit, 1991), and the resulting ethanol yield is less than the other processes. Therefore, this process is unsuitable for commercial production

1.2.2 Continuous fermentation

In the past, ethanol fermentation process from sugar cane molasses was carried out using batch mode (Sanches *et al.*, 1996). However, 30% of the industries have substituted batch by continuous fermentation process (Wheals *et al.*, 1999) because this process provide several advantages. High ethanol productivity was achieved with a medium containing 10%, w/v sucrose at a dilution rate of 0.20 h⁻¹. Moreover, glucose was converted to ethanol by calcium-alginate-entrapped *S. cerevisiae* NRRL Y-2034 cells in continuous-flow and static repeated-batch fermentors. In most cases, the continuous fermentations were produced maximum ethanol yields (3.11 g/10g of glucose) over extended time periods (McGhe *et al.*, 1982)

This process resulted in improvement of the productivity, and increase ethanol yield (Ranulfo *et al.*, 2003). However, the effluent stream can cause a major loss of the biocatalyst, especially when the specific growth rate is low, and the dilution rate (D) is

high. In addition, controlling steps during operation for both *chemostat* and *turbidostat* are difficult. In a *chemostat* the liquid volume is kept constant by setting the inlet and outlet flow rate equal; the dilution rate is therefore constant and steady state is achieved by concentrations in the chemostat adjusting themselves to the feed rate. In a *turbidostat*, the liquid volume is kept constant by setting the outlet flow rate equal to the inlet flow rate; however, the inlet flow rate is adjusted to keep the biomass concentration constant. Thus, in a turbidostat the dilution rate adjusts to its steady-state value corresponding to the set biomass concentration. Turbidostats require more complex monitoring and control systems than chemostats and are not used in large scale (Doran, 1995).

1.2.3 Fed-batch fermentation

It is essential to keep the culture volume constant in continuous operation, whereas there is volume variation in the fed-batch process (Caylak and Sukan, 1998). The fed-batch operation, which may be regarded as a combination of the batch and continuous operations, is by far the most popular in the ethanol industry. The system can be operated with high cell concentration resulting in high volumetric productivity. In fed-batch culture *S. cerevisiae* cells gave the maximum ethanol productivity $3.8 \text{ g.L}^{-1}.\text{hr}^{-1}$ at an initial sugar concentration of 250 g.L^{-1} (Roukas, 1996). However, main advantages of the fed-batch system are that substrate/product inhibition and catabolite repression can be prevented by intermittent feeding of the substrate, in addition; this process can be minimize the cost associated with the inoculum preparation step (Converti *et al.*, 2003). Thus, this thesis will be focused on fed-batch fermentation process.

Because of the progressive change in the broth volume (V), the feed flow rate

(F) of a fed-batch process can be defined as;

$$F = \frac{dV}{dt} = F_0 e^{Kt} \quad (1)$$

Where, F_0 is the starting flow rate, t is the fermentation time, and K is a time parameter on which the flow rate pattern. The value of K can be 0, $K < 0$ or $K > 0$ which correspond to constant feeding rate, exponentially decreasing and increasing flow rate, respectively. Modelling of a fed-batch process should consider the continuous variation of all kinetic parameters during fermentation due to volume variation, mass balance equations for biomass, substrate, and dissolved oxygen, and mass transfer (Di *et al.*, 2001). However, the resulting system of differential equations does not allow analytical solutions, especially when the flow rate continuously varies. Hence, in order to provide a set of equations easily and rapidly applicable to predict the behaviour of industrial fed-batch fermentations, average values of the main kinetic parameters and yields between the starting and final states of each run were used (Converti *et al.*, 2003). Such a simplified approach was utilized with success in studies dealing with the influence of operating conditions on kinetics and yields of different fermentations, during which they varied along the time as well.

Previous work (Carvalho *et al.*, 1993) revealed that the average productivities of biomass, r_x , and ethanol, r_E , were Monod-type functions of the starting substrate-feeding rate

($F_0 S_0$):

$$r_x = \frac{X_f V_f - X_0 V_0}{V_f t_f} = \frac{r_x^{\max} F_0 S_0}{k_x + F_0 S_0} \quad (2)$$

$$r_E = \frac{E_f}{t_f} = \frac{r_E^{\max} F_0 S_0}{k_E + F_0 S_0} \quad (3)$$

where X_0 and S_0 were the starting concentration of biomass and the substrate concentration in the feeding mash, X_f and E_f were the final concentrations of biomass and ethanol, r_X^{\max} and r_E^{\max} were the maximum values of r_X and r_E , and k_X and k_E the corresponding saturation constants, respectively. In addition the substrate consumption rate (r_S) can be defined as

$$r_S = \frac{S_0(V_f - V_0)}{V_f t_f} \quad (4)$$

Correspondingly, the yields of biomass on substrate ($Y_{X/S}$), ethanol on substrate ($Y_{E/S}$) and biomass on produced ethanol ($Y_{X/E}$) were calculated as the ratios of their respective rates:

$$Y_{X/S} = \frac{r_X}{r_S} = \frac{X_f V_f - X_0 V_0}{S_0(V_f - V_0)} \quad (5)$$

$$Y_{E/S} = \frac{r_E}{r_S} = \frac{E_f V_f}{S_0(V_f - V_0)} \quad (6)$$

$$Y_{X/E} = \frac{r_X}{r_E} = \frac{X_f V_f - X_0 V_0}{E_f V_f} \quad (7)$$

1.3 Technical problems for the production of high purity ethanol

Despite the obvious importance of this process, physiological constraints limit the rate of glycolysis and ethanol production (Casey and Ingledew, 1986). Identification of these constraints represents an important step toward the development of improved organisms and process conditions for more rapid ethanol production capacity of existing

fermentation plants, and a reduction in the cost of future facilities (Dombek and Ingram, 1985).

1.3.1 Problems from biocatalyst

The first problem arises from the biocatalyst itself. Yeast is highly susceptible to ethanol inhibition, and the product yield attained in practical fermentations never exceeds 90 – 95% of the theory. Concentrations of 1-2% (w/v) are sufficient to retard microbial growth and at 10% (w/v) alcohol, the growth rate of the organism is nearly halted (Krauter *et al.*, 1987). Inhibition effect occurred by the ethanol could even result in cell death (Echegaray *et al.*, 2000). Ethanol is known to alter membrane permeability and disrupt membrane function in a variety of biological systems. In yeasts, ethanol causes an increase in hydrogen ion flux across the plasma membrane of cells suspended in water (Cartwright *et al.*, 1986). This increased hydrogen ion flux has been proposed as being responsible for the ethanol-induced decline in transport rates observed under similar condition (Beavan *et al.*, 1982).

1.3.2 Purification problems

The second constraint associates with engineering problems for the productions, recovery, and purification processes. Ethanol is normally purified by distillation of aqueous solutions, and the initial concentration in the fermentation broth is between 5 to 10%. However, pure ethanol cannot be obtained by the mean of simple distillation. Ethanol forms an azeotropic solution (close boiling point mixture) with water at the concentration of 95.6 (%w/w), and distillation becomes ineffective removing the trace amount of water. Azeotropic distillation with an additive, normally either cyclohexane or benzene, needs to be accomplishing (Matsuura, 1994). Therefore, commercial ethanol

contains 95 percent by volume of ethanol and 5 percent of water whilst dehydrating agents can be used to remove the remaining water, and produce absolute ethanol (Lye and Woodley, 1999). In conclusion, production of high purity ethanol using conventional aqueous distillation is complicate and energy consuming process; thus, make the commercialization difficult and not economically feasible. Nowadays, most of high purity ethanol have to be imported from abroad due to too high production cost, and the selling price in the country (about 15 baht per litre) is not attractive (Thairath, 2548).

1.4 Extractive Fermentation

As mentioned earlier, accumulation of ethanol in the fermentation broth plays a major role in stopping the yeast's activity at the end of the process. Extractive fermentation was therefore developed as a process to overcome with the phenomenon of end product inhibition. It is a processing strategy in which reaction and recovery occur simultaneously in a bioreactor through the use of a water-immiscible, biocompatible solvent which selectively removes the inhibitory product. There are many techniques for extractive fermentation or *in situ* product removal including pervaporation, gas stripping, aqueous organic two phase system and perstraction system. Firstly, gas separation membranes, the separation are usually based on dissolution and diffusion behavior. The gas to be dried should be fed to the retentate side at a high pressure and/or a partial vacuum should be applied to the permeate side in order to obtain sufficient driving force for the transport of water through the membrane. A disadvantage of this procedure is the usually relatively very high volume of the permeate compartment which is necessary to counteract pressure loss and, consequently, loss of driving force. Another important disadvantage is the-frequently high loss of gas to be dehydrated, which occurs through

permeation together with the water vapor. If gases are dehydrated under increased pressure, the gas separation membranes have to have a high mechanical strength in order to be resistant to this high pressure(database, 2006).

Subsequently, aqueous organic two phase system (AOTPs) comprise a freely suspended biocatalyst dispersed in an aqueous phase, and contain an organic solvent as the second phase which acts as a reservoir for the substrate and biotransformation products due to the high solubility of these solutes in the organic phase. Using this technique, it is possible to introduce high substrate concentrations as well as achieve a high concentration of products in the organic phase. The substrate will be gradually released from the organic phase into the aqueous phase to react with the biocatalyst, and the product will partition back into the organic phase. The implementation of this system protects the micro-organism from substrate and product toxicity(Leon *et al.*, 1998), and also prevent auto-oxidation of the products in the aqueous phase. Many studies have been carried demonstrating the advantages of the system in term of controlling substrate toxicity and achieving high product concentration in the organic phase (Van Keulen *et al.*, 1998). The system forms this system, and the products partitioned into the organic solvent can be recovered by distillation or back extraction. The solvent comprised substantially of long chains alcohol, which has a high affinity for ethanol, is continuously introduced to the bioreactor. Essentially, the solvent is non-volatile, non-toxic and is recovered for reuse in the bioreactor (Ann, 2000). 1-Decanol was used as the extractants within reactors designed specifically for extractive fermentations, and improved productivities have also been demonstrated within less specialized reactors to produce ethanol (Mattiasson and Holst, 1991).

However, the biocompatibility of micro-organism with the organic solvent is an important parameter in overcoming substrate toxicity to the cell. Although an aqueous organic two phase system results in a number of the advantages for biotransformation, some problems arise from this system, particularly the formation of emulsion resulting from biological surfactants which cause major difficulties for further product recovery (Boontawan, 2005). In addition, major saving cost in the extractive process resulted from usage of smaller bioreactor due to increased bioreactor productivity, and from reduced energy and capital requirements in the stillage-handling section of the plant due to reduced water requirements.

1.5 Membrane separation processes

In parallel with fermentation kinetic studies, the use of membranes to extract fermentation products from the aqueous phase was introduced many years ago in order to improve the traditional production processes (Doig *et al.*, 1998). In our particular system, membrane separations are the most effective techniques. Membrane separation has been widely used for purification concentration of fluid mixtures. Theory of membrane transport is concerned with chemical nature of the membrane, physical structure and physio-chemical properties of the mixture to be separation. The main interest will be focused on the absorption of organic compounds into the membrane surface and the diffusion of them in the membrane matrix (Li *et al.*, 2000).

Concerning ethanol fermentation, most research works on removal of ethanol from fermentation broths or ethanol/water mixture have been accomplished using pervaporation technique (Giorno and Drioli, 2000). Pervaporation is a membrane separation process in which vacuum is applied to the downstream side of the membrane.

Separation occurs through the combination of a difference in permeation rates of ethanol and water molecules through a non-porous, semi-permeable membrane. An evaporative phase change somewhere between the upstream and downstream sides of the membrane; as a result, the permeate will be obtained as gaseous vapor which needs to be condensed prior to further distill (Huang, 1991). The membrane should have the required separation properties, which is a high permeation rate for ethanol, but low for water. Membranes with extremely thin selective barriers with the necessary mechanical strength are obtained by producing composite structure. These membranes consist of a 0.1-5 μm thick homogeneous polymers film (dense membrane) deposited on a microporous support structure (Mattiasson and Holst, 1991). The primary benefit of an integrated fermentation-ethanol recovery process is therefore a greatly increased volumetric productivity which translates to less installed bioreactor capacity. Pervaporation may have advantages over other techniques in terms of simplicity of the process; prevent toxicity to fermenting organisms, and recovery of a concentrated ethanol stream requiring less distillation capacity and energy consumption. Nevertheless; disadvantages of pervaporation would include the need for low temperature condensation of permeate vapors (Taylor *et al.*, 1995), and the permeate still forms an azeotropic solution. In the previous study, indicated that in fed-batch fermentations from corn fiber hydrolysate the ethanol yields and final ethanol concentration of the two hydrolysates were similar at 0.32-0.43 g/g and 29-44 g/l, respectively. Coupling of a membrane pervaporation unit to a fed-batch fermentation of hydrolysate maintained the ethanol concentration below 25 g/l with complete sugar utilization. A concentrated ethanol stream of 17 wt.% ethanol was produced by the pervaporation unit (O'Brien *et al.*, 2004).

Moreover, the fermentation-pervaporation system requires a refrigeration plant to condense the vapors from the pervaporation unit. Technical feasibility needs to be demonstrated in significant pilot plant studies. The energy consumption of this dehydration process is very high, and a new process to reduce the dehydration cost has been sought for (Matsuura, 1994). The most widely study of ethanol separation is perstraction system. Thus, this study will focus on membrane in liquid-liquid contacting system as a separation unit (perstraction) coupling with a continuous production in a bioreactor in order to obtain uncontaminated, and “ethanol-rich” organic solvent. Fermentation-Perstraction system mainly concentrates on the integration of upstream and downstream processing. Since ethanol molecule is small (MW 46), dense phase membrane seems to be an ideal for separation from the fermentation broth. In addition, this technique is used to prevent the formation of emulsion in aqueous-organic two phase system, and also facilitate further recovery process. Solvent selection should be accomplished mainly on the partition coefficient because these values strongly affect to the solvent requirement and the cost of process. Ethanol-extracting capacity of long chain alcohol is the highest compared with ether, ketone, ester, etc. 1-decanol is long chain alcohol (C₁₀) and they are highly hydrophobic. However, some solvent may be soluble in ethanol, and more expensive (Mattiasson and Holst, 1991). Thus, 1-decanol is the most suitable for separation of ethanol/water mixture, and will be used as the extractant for this work.

1.5.1 Transport mechanism of hydrophobic solutes through silicone rubber membrane in a liquid-liquid contacting system

Since mass is transferred from one location to another under the influence of a concentration difference in the system and more importantly the interaction between the

solute and polymer, the first step in evaluating the feasibility of membrane separation in a liquid-liquid contacting system is to measure the solubility, or membrane-aqueous partition coefficient, of the organic compounds in the membrane phase (Pauline, 1995).

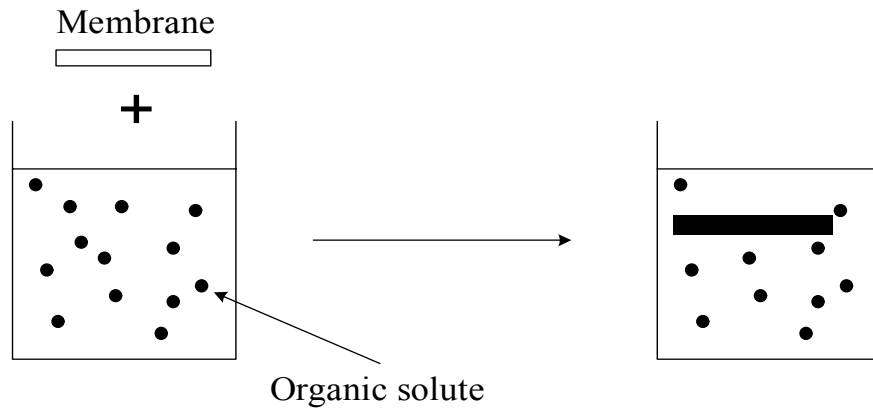


Figure 2 Absorption of organic molecules in the membrane matrix.

Figure 2 depicts the absorption process of an organic compound into the matrix of a membrane matrix. When a section of membrane free from organic solutes is submerged in a dilute solution of organic compounds, hydrophobic interactions result in a partitioning of the organic molecules into the membrane matrix (Huang, 1991). The solute then diffuses through the membrane, and equilibrium occurs when the rate of solute absorbed into the membrane equals the desorption rate. If there is no loss of solute due to evaporation or absorption into other contacting materials, a decrease in organic solute concentration results from this partitioning into the membrane, and the membrane/aqueous partition coefficient (P_{aq}^{mem}) can be defined as the ratio of solute concentration in the membrane (C_{mem}) and aqueous phase (C_{aq}). Hence;

$$P_{aq}^{mem} = \frac{C_{mem}}{C_{aq}} \quad (8)$$

In addition, non-steady state organic solute absorption kinetics can be measured to obtain the diffusivity of the organic solute in the membrane. A plot of time, and the ratio of organic solute absorbed into the membrane at time = t and at equilibrium can be used to estimate membrane diffusivity by a late-time approximation equation as follows (Crank, 1979);

$$\frac{M_t}{M_\infty} = 1 - \frac{8}{\pi} \exp\left[-\frac{\pi^2 D_{mem} t}{\delta^2}\right] \quad (9)$$

Where M_t is the mass of organic solute absorbed in the membrane at time = t, D_{mem} is the membrane diffusivity, and δ is the membrane thickness. From the above equation, a plot of $-\ln(1-M_t/M_\infty)$ against t results in a straight line from which the diffusivity (D_{mem}) can be deduced from the slope.

The mass component transported across the membrane per unit area per unit time (mass flux, J_i) can be defined using Fick first's law of diffusion which depends on the overall mass transfer coefficient. Fick developed the law of diffusion with Fourier's work (Cussler, 1997). The solution-diffusion model is by far the most popular model to explain permeation characteristic of the organic solutes through the membrane (Wijmans and Baker, 1995). The transport rate of component i through the membrane governed by Fick's law of diffusion is;

$$J_i = -D_i \frac{d\chi_i}{d\delta} \quad (10)$$

Where; $d\chi_i/d\delta$ is the chemical potential gradient of component i across the membrane, δ is the thickness of the membrane, and D_i is the diffusion coefficient, respectively. In addition, the rate of mass transfer is directly proportional to the driving force for transfer and the area available for the transfer process to take place. The proportionality coefficient in this equation is therefore called the mass transfer coefficient (k_{ov}), so that;

Mass transfer rate = (mass transfer coefficient) \times (transfer area) \times (driving force)

$$-N_i = k_{ov}A\Delta C \quad (11)$$

Since this is the three aqueous-membrane-organic phase system; therefore, there are three main resistances that contribute to the overall resistance namely aqueous phase (k_{aq}), membrane (k_{mem}), and organic phase resistance (k_{org}) respectively. The theoretical aqueous and organic boundary layer and the membrane resistance are shown in Figure 3. At the first stage, organic solvent will be migrated into the membrane matrix due to hydrophobic-hydrophobic interaction, and the aqueous-organic phase boundary interface is subsequently formed at the aqueous side of the membrane. The organic solute is then absorbed into the surface of the membrane due to high partition coefficients (P_{aq}^{mem} and P_{aq}^{org}). Base on the two-film theory of Whitman, it is assumed that turbulence dies out just before the fluid interface resulting in a stagnant boundary layer on both sides of the liquid-liquid interface. In the bulk region outside the laminar layer represented by the dashed lines, turbulent eddies supplement the mass transfer caused by random movement of the hydrophobic solute, and the resistance to mass transfer becomes significantly smaller (Cussler, 1997). When the membrane is used to contact the two liquids phase, it is considered as a distinct phase from the two liquid phases. Once the

solute concentration in the membrane is built up, concentration difference (ΔC) occurs and generate a driving force which responsible to the diffusion across the membrane prior to desorbed into the organic phase (Livingston, 1994).

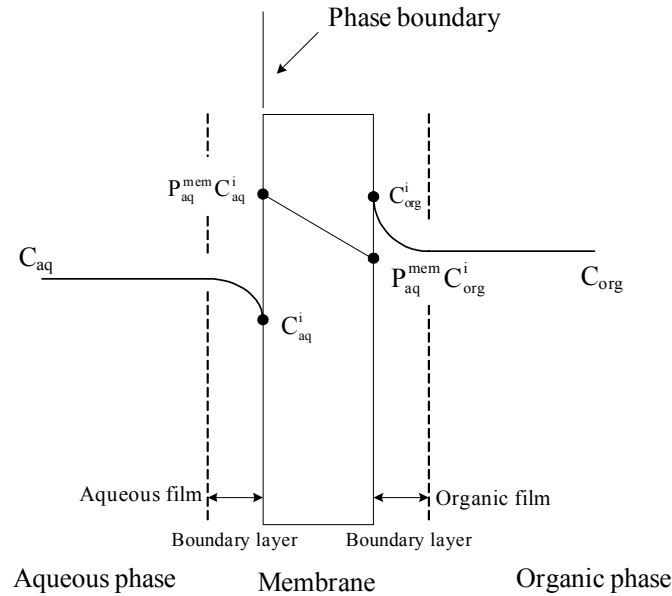


Figure 3 Concentration profile of organic solute in a hydrophobic membrane organic-aqueous two phase system (Boontawan, 2005).

Transport through layer of a composite membrane can be widely accepted using solution-diffusion model (de Pinho *et al.*, 1990). Under equilibrium conditions, organic solute concentrations in the three distinct phases can be described by partition coefficients as follows;

$$\text{Organic/aqueous partition coefficient; } P_{\text{aq}}^{\text{org}} = \frac{C_{\text{org}}}{C_{\text{aq}}} \quad (12)$$

$$\text{Membrane/aqueous partition coefficient; } P_{\text{aq}}^{\text{mem}} = \frac{C_{\text{mem}}}{C_{\text{aq}}} \quad (13)$$

$$\text{Membrane/organic partition coefficient; } P_{\text{org}}^{\text{mem}} = \frac{C_{\text{mem}}}{C_{\text{org}}} \quad (14)$$

A number of mathematical equations have been formulated based on Fick's law using different for concentration dependence of solubility or diffusivity (Jiratananon *et al.*, 2002). In perstraction system, the total flux of component i (J_i) is actually the combination of the total mass flux from the bulk aqueous phase (C_{aq}) to the bulk organic phase (C_{org}) which includes the aqueous boundary layer of the absorption side (J_{aq}^i), diffusion flux through the membrane matrix (J_{mem}^i), and desorption flux to the organic solvent (J_{org}^i). The rate of mass transfer J_i in each phase can then be defined as follows;

$$-J_{aq}^i = k_{aq}(C_{aq} - C_{aq}^i) \quad (15)$$

$$-J_{mem}^i = k_{mem}(P_{aq}^{mem}C_{aq}^i - C_{org}^i) \quad (16)$$

$$-J_{org}^i = k_{org}(C_{org}^i - C_{org}) \quad (17)$$

At steady state, the overall mass transfer rate of organic solutes through the system (J_i) is equal to the rate through aqueous film, membrane matrix, and organic film respectively ($J_{aq}^i = J_{mem}^i = J_{org}^i = J_i$). Therefore, we can rearrange equation (10), (11), (12) and eliminate of interfacial concentrations by combination of all equations, and give;

$$-J_i \left(\frac{1}{k_{aq}} + \frac{1}{k_{mem}P_{aq}^{org}} + \frac{1}{k_{org}P_{aq}^{org}} \right) = C_{aq} - \frac{C_{org}}{P_{aq}^{org}} \quad (18)$$

Therefore, the correlation between k_{ov} and the individual resistances can also be derived in the same way as the thermal resistances in series model. Hence;

$$\frac{1}{k_{ov}} = \frac{1}{k_{aq}} + \frac{1}{k_{mem}P_{aq}^{org}} + \frac{1}{k_{org}P_{aq}^{org}} \quad (19)$$

For the membrane resistance (k_{mem}), the permeability of the hydrophobic molecules through the membrane is governed by three parameters which are membrane/aqueous partition coefficient (P_{aq}^{mem}), membrane thickness (δ) and the membrane diffusion coefficient (D_{mem}). Thus, the above equation can be re-written as;

$$\frac{1}{k_{ov}} = \frac{1}{k_{aq}} + \frac{\delta}{D_{mem} P_{aq}^{mem} P_{aq}^{org}} + \frac{1}{k_{org} P_{aq}^{org}} \quad (20)$$

In order to minimize the overall resistance (maximize the k_{ov}), study of individual parameters are required. The influence of k_{aq} and k_{org} to the k_{ov} can be studied by varying the hydrodynamic conditions of both aqueous and organic phase, and they were well investigated. The effect of organic Reynolds number (Re_{org}) was negligible to the k_{ov} due to high diffusivity of the solutes in the organic solvent (Doig *et al.*, 1999). In conclusion, the effect of Re_{org} to the overall mass transfer coefficient is negligible, and the system can be operated at low Re_{org} in order to minimize the size of a pump, and electricity cost. However, aqueous phase Reynolds number (Re_{aq}) had a profound effect to the k_{ov} . This is due to the existence of theoretical boundary layer in the aqueous side of the membrane in which the mass transfer across this layer occurs by conductive flow (diffusion) only. However, operation at turbulent regime is enough to keep the k_{aq} at the minimum effect. Therefore, the main resistance contributed to the overall resistance is related primarily to membrane thickness and diffusive permeability. For a given system, permeability of organic through the membrane is governed by the magnitude of membrane/aqueous partition coefficient. Therefore, in an attempt to minimize mass transfer resistance related to the membrane, manufacture of composite membranes have made a concerted effort to reduce wall thicknesses (William and James, 2000). So, this research will be emphasized on a development of a fabrication technique to produce an extremely thin

selective layer on a porous support (composite membrane) in order to minimize the membrane resistance.

1.6 Composite PDMS/PVDF membrane

Membrane thickness often plays an important role on the mass transfer characteristic of solutes across the membrane. Manufacturing of a composite membrane, which combines the separation properties of a coating material and the mechanical strength of a supportive layer, could provide high k_{ov} due to its extremely thin selective layer, and can reduce the membrane area needed for the fermentation process (Ho and Sirka, 1992). Numerous researches have focused on the fabrication of composite membranes with an extremely thin selective layer, with an approximate thickness of around 10-15 μM , on the top of a highly porous supporting layer with reasonably small pore sizes. One of the most popular techniques is the coating of silicone rubber, usually polydimethylsiloxane (PDMS), on an asymmetric polyvinylidene fluoride (PVDF) membrane.

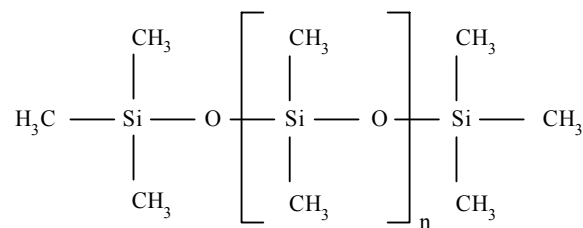


Figure 4 Chemical structure of polydimethylsiloxane polymer (PDMS)

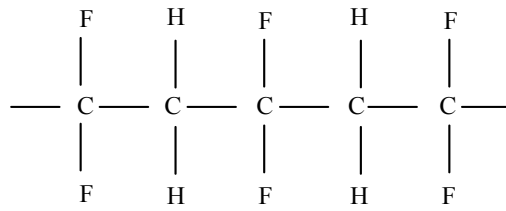


Figure 5 Chemical structure of polyvinylidene fluoride (PVDF)

The thin film polymer exhibits hydrophobicity, and allows the organic molecules to permeate across the membrane, whilst the asymmetric flat sheet PVDF supporting membrane provides mechanical support for the thin film coating (Daisley *et al.*, 2006). Ideally, the thin film layer should provide good permeability to organic compounds, and is supported by a thick porous sub-layer. The first step in constructing the membrane module involves the fabrication of an asymmetric flat sheet PVDF layer. Asymmetric membranes are layered structured in which the porosity, pore size or composition change from the top to the bottom surface of the membrane (Baker, 2004). The top surface usually possesses a thin, very finely micro-porous structure whilst the bottom layer has finger-like void structure which extended from just under the dense skin to the bottom surface. Figure 6 shows the schematic diagram of a composite PDMS/PVDF membrane. The supportive layer can be fabricated using hand-casting knife. Casting solution is usually prepared from 14% (w/v) polyvinylidene fluoride or polysulfone in N-methylpyrrolidone as the organic solvent, and a non-solvent additive (LiCl) (Wang *et al.*, 2000). A dry-wet phase inversion technique is employed to prepare this asymmetric membrane. A short exposure of the mixture polymer to the air (drying process) allows the solvent and/or non-solvent additive to evaporate from the surface prior to coagulation in a water

bath (wet process). The silicone rubber can then be coated on the supportive layer prior to test for the separation performance of the ethanol/war mixture.

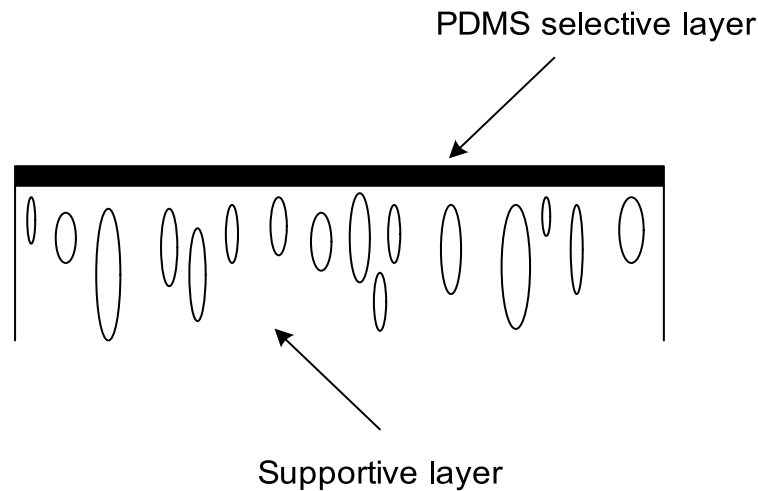


Figure 6 Schematic diagram of PDMS/PVDF composite membrane casting from dry-wet phase inversion technique showing the dense top layer and finger-like void structure at the bottom.

1.7 Membrane bioreactor for continuous separation of organic solutes from the fermentation broth

The use of membranes to extract biotransformation products from the aqueous phase was introduced many years ago in order to improve the traditional production processes. It combines *in situ* product mass transport from the reaction site with biochemical reactions (Giorno and Drioli, 2000). Continuous product removal increases the conversion of product-inhibited biochemical reactions, and the products in the permeate side can be processed separately and efficiently (Lye and Woodley, 1999). This *in situ* product removal technique could result in much higher volumetric productivity compared to a conventional fermentation process (Boontawan, 2005). In addition, the separation of products from other bioreactor constituents is often difficult, and is a costly step in large-scale industrial bioprocesses. A proposed principle of fermentation-

perstraction membrane bioreactor can be given in Figure 7. Yeast consumes sugar (substrate) in order to produce ethanol (product) which is subsequently absorbed into the membrane. Diffusion and desorption are the major step to obtain pure ethanol in the organic reservoir. A simple distillation can be employed to obtain absolute ethanol, and the remaining organic solvent can be reused. Thus, the main advantages for this study are to obtain “ethanol-rich” organic solvent, minimize the total downstream processes, reduce the toxicity to the cell, increase the product yield, recycle the biocatalyst, and make the processes continuous.

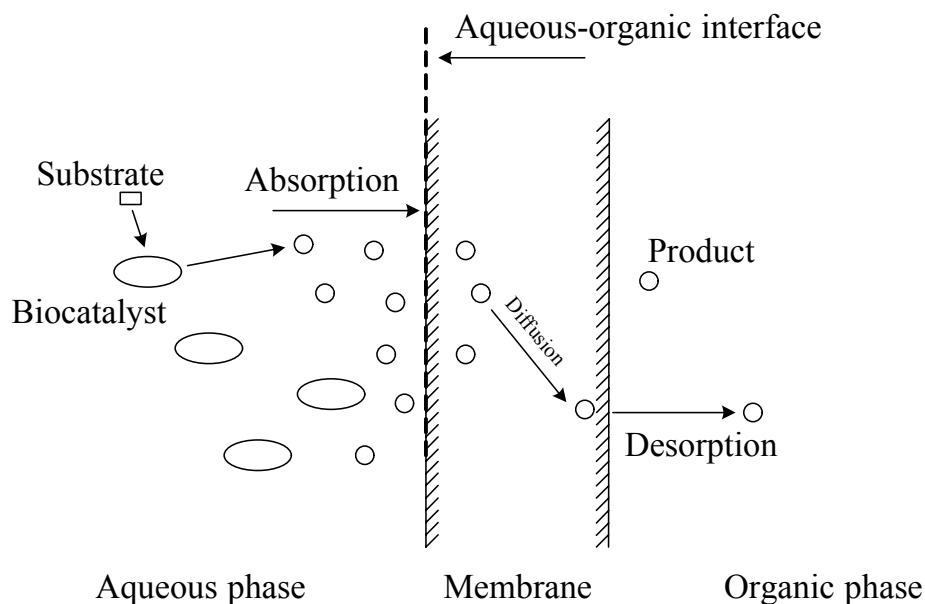


Figure 7 Schematic diagram for the working principle of perstractive membrane bioreactor (Boontawan, 2005).

1.8 Thesis Objectives

1. To obtain high ethanol yield in the fermentation process.
2. To study the application of composite PDMS/PVDF membrane in membrane bioreactor

3. To separate ethanol from fermentation broth using a membrane in Liquid-Liquid contacting system (perstraction technique).

1.9 Scope and limitation of the study

Investigate partition coefficients in order to have an insight into mass transfer characteristic of perstraction system and Mass transfer study of ethanol through silicone membrane will be conducted using amyl alcohol as an organic solvent. The membrane is placed between two o-rings which also provides flow channels, and is housed in two stainless steel plates. Ethanol/aqueous mixture and organic phase will be re-circulated using two gear pumps. This set up allows independent controlling of hydrodynamic effect for both aqueous and organic side. Mass transfer characteristic of ethanol through membrane will be monitored using gas chromatography technique. Study previous reviewed literatures of ethanol synthesis pathway by *S. cerevisiae* including fermentation kinetics and toxicity effect to the yeast cell. Finally, combination of ethanol fermentation and *in situ* product removal via perstraction technique will then be performed. The system performance will then be compared with conventional ethanol fermentation.

1.10 Expected results

1. The high yield of ethanol in this fermentation will be obtained.
2. The perstraction techniques for separation of ethanol from fermentations will be obtained.
3. The suitable membrane for extraction of ethanol from fed-batch fermentation with *in situ* ethanol removal will be obtained.

CHAPTER II

MATERIALS AND METHODS

2.1 Chemicals

Polyvinylidene fluoride (PVDF) was a gift from Arkema (Thailand). Two types of Polydimethylsiloxane (PDMS) were kindly provided by Dow Corning (Thailand), and Rhodia (Thailand). Analytical grade of pentanol, 1-decanol, and 1-methyl-2-pyrrolidone were purchased from Fluka (United Kingdom). Molasses and commercial yeast (*S. cerevisiae*) were purchased from a local supplier. Other chemicals were all of reagent grade.

2.2 Membrane preparation and characterization

2.2.1 Preparation of PDMS, and composite PDMS/PVDF membrane

Various thicknesses of PDMS membrane (2 μm , 100 μm , 300 μm) were prepared by solution casting technique. Masses of PDMS were dissolved in hexane (10%, w/v) prior to add catalyst. The solutions were then casted on Teflon[®] coated plate. Hexane was then evaporated and thin films of PDMS were formed under ambient condition. For preparation of composite membrane, polyvinylidene fluoride (PVDF) membrane as the support layer was firstly fabricated by hand-forming using dry-wet phase inversion

method. The dope composition was detailed as followed; 15 % PVDF in 85 % N-methyl pyrrolidone (NMP)(wt/wt) and 4 g of lithium chloride (LiCl) was added in every 100 g of PVDF-NMP solution as non-solvent additive (Kong and Li, 2001). After the PVDF support layer was formed, the PDMS solution was then poured on top and extremely thin layer of PDMS was formed. Scanning Electron Microscope (SEM) was then employed to characterize the structure of casted membranes.

2.2.2 Membrane/aqueous partition coefficient, P_{aq}^{mem}

Varying masses of the membranes saturated with either pentanol or 1-decanol were put into a series of sealed glass tubes containing 25 mL of a known ethanol concentration in an aqueous phase (ethanol/water mixture). It was then incubated at temperature of 30°C for 24 hours. After incubation, gas chromatography was used to determine the concentration left in aqueous phase. The mass balance can be written as;

$$V_{aq} C_0 = V_{aq} C_{aq} + V_{mem} C_{mem} \quad (21)$$

Where V_{aq} is the volume of aqueous phase (m^3), V_{mem} is the volume of membrane phase (m^3), C_0 is the initial concentration of solute in the aqueous phase ($kg.m^{-3}$), C_{aq} is the equilibrium concentration of the organic solute in aqueous phase ($kg.m^{-3}$), and C_{mem} is the equilibrium concentration of solute in the membrane phase ($kg.m^{-3}$). Moreover, $P_{aq}^{mem} = C_{mem}/C_{aq}$, it then be combined with the two sides of the above equation and gives;

$$\frac{C_0}{C_{aq}} - 1 = P_{aq}^{mem} \times \frac{V_{mem}}{V_{aq}} \quad (22)$$

A plot of $V_{\text{mem}}/V_{\text{aq}}$ versus $C_0/C_{\text{aq}} - 1$ were result in a straight line, the slope of which were give an estimated value of $P_{\text{aq}}^{\text{mem}}$ (Livingston, 1994).

2.2.3 Organic/aqueous partition coefficient, $P_{\text{aq}}^{\text{org}}$

Two equal volumes of organic solvent (1-decanol) and ethanol/water mixture were put together in small tube. The tube were shaken vigorously for 5 minutes and incubated at temperature of 30°C for 24 hours. The aqueous/organic partition coefficients of the chemicals were then calculated from the ratio of the organic phase and aqueous phase concentration. Addition, the determined of $P_{\text{aq}}^{\text{org}}$ by using gas chromatography (Doig, 1998). Table reveals some important properties of pentanol and 1-decanol.

Table 3 Physio-chemical properties of the organic solvents used in this study.

Physio-chemical properties	Pentanol	1-Decanol
Formula	$C_5H_{12}O$	$C_{10}H_{22}O$
Molecular weight	88	158.28
Specific gravity	0.811	0.83
Boiling point (°C)	138	230
Melting point (°C)	-78	7
Solubility (g/100mL, 20 °C)	2.70	0.37

2.2.4 Absorption and diffusivity of ethanol in PDMS

Silicone sheets were cut and weight to 0.2 g before being placed in 1.5 ml of known concentration of aqueous mixture in a glass tube. The samples were incubated in a rotary shaker at 250 rpm and the temperature was set at 30°C to ensure a homogeneous condition throughout the experiment. Concentration in the aqueous phase was

periodically measured until it reached a constant value. Assuming that there is no adsorption into the glass wall, the diminishing concentration in the aqueous phase of ethanol was only due to adsorption into the membrane. Due to the high hydrophobicity of the membrane material, absorption of water very low and can be considered as negligible. The mass of ethanol absorbed into the silicone membrane can simply be calculated as;

$$M_t = (C_0 - C_t)V \quad (23)$$

Where M_t is the mass of ethanol absorbed into the membrane, C_0 is the initial concentration of solution, C_t is the concentration of ethanol at time = t , and V is the volume of the solution. The error associated with the determination of absorption measurement was $\pm 3\%$ quoted at the 95% confidence interval of 3 repeated experiments.

2.3 Experimental setup and mass transfer study

2.3.1 Membrane module

Figure 8 and Figure 9 detail the schematic diagram of the membrane module, and mass transfer experimental setup employed in this work. The module was consisted of a flat-sheet membrane (either composite or flat-sheet) placed between two rubber gaskets which provide flow passage, and was housed between two plates constructed from stainless steel. Two hot plate stirrers (Biosan, MSH 30) were employed to regulate the two liquid temperatures, and also maintain its homogeneity. Organic phase was re-circulated using a variable speed gear pump (Cole Palmer, USA) whilst aqueous solution was re-circulated using a peristaltic pump (Watson Marlow, UK).



Figure 8 Schematic diagram of the perstraction membrane module used in this study

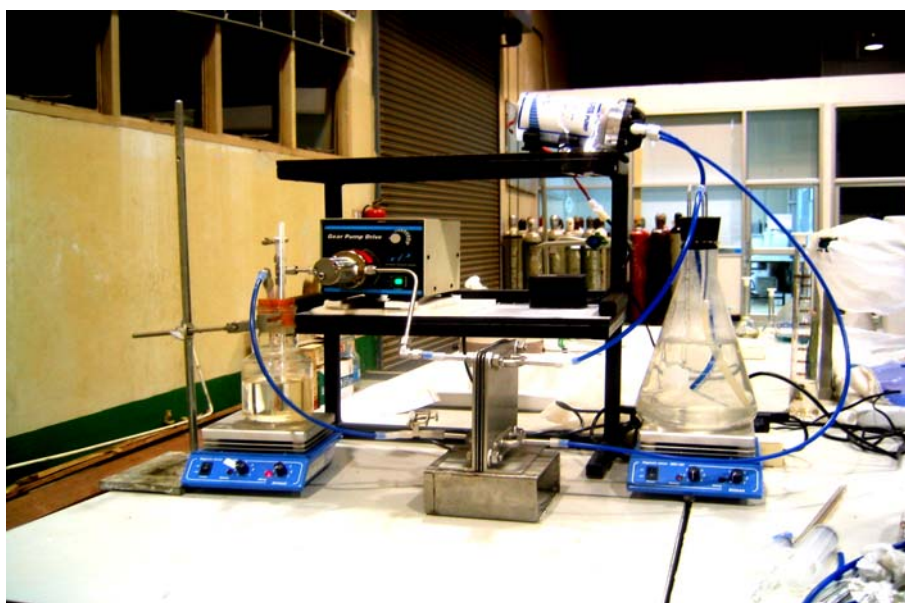


Figure 9 An experimental set up for separation of ethanol from diluted aqueous solution

2.3.2 Transport mechanism of ethanol through PDMS membrane.

The aqueous phase flow rate was varied using a variable speed peristaltic pump, whilst the organic flow was controlled by a gear pump. The Reynolds numbers were defined as (Doig, 1998);

$$Re = \frac{\rho d^{HR} u}{\mu} \quad (24)$$

Where; ρ is the fluid density (kg.m^{-3}),

d^{HR} is the hydraulic diameter which is $4 \times \frac{\text{hydraulic surface area}}{\text{wetted perimeter}}$,

u is the bulk fluid velocity (ms^{-1}) and μ is the viscosity of the fluid.

Graphical determinations of the overall mass transfer coefficient (k_{ov}) were accomplished using a modified equation of Fick's law (Boontawan, 2005). Assuming that pseudo-steady state occurred, there was no accumulation of ethanol in the membrane, and the two liquid phases were well mixed. The process for organic solutes transferring from the aqueous phase to organic solvent can be given by;

$$V_{org} \frac{dC_{org}}{dt} = k_{ov} A \left[C_{aq} - \frac{C_{org}}{P_{aq}^{org}} \right] \quad (25)$$

Because;

$$V_{org} C_{org} = V_{aq} (C_{aq}^0 - C_{aq}) \quad (26)$$

Then;

$$C_{aq} = C_{aq}^0 - \frac{V_{org} C_{org}}{V_{aq}} \quad (27)$$

Therefore;

$$V_{org} \frac{dC_{org}}{dt} = k_{ov} A \left[\left(C_{aq}^0 - \frac{V_{org} C_{org}}{V_{aq}} \right) - \frac{C_{org}}{P_{aq}^{org}} \right] \quad (28)$$

Rearrangement of the above equation gives;

$$V_{org} \frac{dC_{org}}{dt} = k_{ov} A \left[C_{aq}^0 - C_{org} \left(\frac{V_{org}}{V_{aq}} + \frac{1}{P_{aq}^{org}} \right) \right] \quad (29)$$

Let,

$$\xi = \frac{V_{\text{org}}}{V_{\text{aq}}} + \frac{1}{P_{\text{aq}}^{\text{org}}} \quad (30)$$

Hence;

$$V_{\text{org}} \frac{dC_{\text{org}}}{dt} = k_{\text{ov}} A [C_{\text{aq}}^0 - C_{\text{org}} \xi] \quad (31)$$

Rearrangement and integration of Equation (31) gives;

$$\int_0^{C_{\text{org}}} \frac{1}{(C_{\text{aq}}^0 - C_{\text{org}} \xi)} dC_{\text{org}} = \int_0^t \frac{k_{\text{ov}} A dt}{V_{\text{org}}} \quad (32)$$

Therefore;

$$k_{\text{ov}} t = \frac{-V_{\text{org}}}{\xi A} \ln \left[1 - \frac{\xi C_{\text{org}}}{C_{\text{aq}}^0} \right] \quad (33)$$

As a result, a plot of the time against the right hand side (RHS) of equation (33) yields a straight line where an estimate of k_{ov} can be obtained from the slope of the graph (Boontawan, 2005).

If the mass transfer rate or extraction rate of ethanol from fermentation broth equal to the ethanol production rate, the systems are therefore in reaction limited condition, and there is no accumulation of ethanol in the broth. On the other hand, if the system is in mass transfer limited condition, ethanol will be accumulated in the fermentation broth which could result in inhibition effect to the biocatalyst. Therefore, calculation of membrane area that suitable for the rate of ethanol production is necessary.

2.4 Fermentation of ethanol from molasses

2.4.1 Batch culture

Commercial strain of *S. cerevisiae* was used in this study. Yeast extract-Malt extract medium consisted of 0.3% yeast extract, 0.3% malt extract, 0.5% peptone, and 1% D-glucose (pH 5.5). Regenerated culture from stock culture was transferred to the medium, and was incubated in a rotary shaker at 200 rpm at 30°C for 24 hours. The regenerated culture was then be streaked onto an agar slant, and stored at 4°C for future use. At the commencement of the experiment, culture was taken from agar slant, and regenerate into 10 mL of YM medium. Incubation was taken place in a rotary shaker at 200 rpm at 30°C for 24 hours. Then, the inoculum was aseptically transferred into 90 mL YM medium, and was incubated using the same condition.

2.4.2 Culture condition for the microorganisms in order to achieve high cell concentration in batch culture

A special formulation of YM medium (Triple X concentration, 0.90 L) with glucose concentration of 50 g.L⁻¹ were prepared in a 2 L conventional stirred tank bioreactor (B. Bruan, Germany), and autoclaved at 121°C for 15 minutes before transferring of the seed. An external electric control unit was used to monitor and regulate condition of the broth. Temperature was set at 30 °C, and the impeller speed was maintained at 250 rpm. The pH was measured by a pH combined electrode (Mettler Toledo, Switzerland), and maintained at a set point (5.5) by the automatic addition of acid (1.0 M of H₂SO₄) or base (1.0 M of NaOH). The dissolved oxygen concentration was measured with a polarographic dO₂ probe (Ingold, Switzerland). At the end of the

process, the resulting high cell cultivation (approximately 25 g/L) was kept for further experiment.

2.4.3 Fed-batch fermentation

Direct feeding of molasses was started at the early of the stationary phase (growth stopped) without further aeration. The reason for this was to provide the anaerobic condition. Concentrated molasses was sterilized prior to use without any addition of other chemicals. Constant molasses feeding rates were carried out between 0.004-0.02 g/s/g_{cell} in order to set up an optimum feeding rate.

2.5 Membrane bioreactor setup for *in situ* ethanol removal in fed-batch fermentation

The regenerated culture from agar slant in YM medium was transferred to the bioreactor. The inoculum sizes were a volume equivalent to 10% of the working volume. The fermentation medium was sterilized at 121 °C for 15 min. The culture pH is automatically controlled at desired values (5.5) by addition of 2M NaOH. The bioreactor was operated under anaerobic condition, agitation at 250 rpm, and temperature at 30°C. Impeller speed was monitored, and regulated using an external electric control unit. Fed-batch fermentation of ethanol coupling with an external perstraction membrane module was operated as shown in Figure 10. Fermentation broth was re-circulated across the feed side of the membranes by a peristaltic pump. The Reynolds number (Re_{aq}) was maintained at 4000 in order to minimize boundary layer effect in the aqueous phase. Organic solvent was also re-circulated at Reynolds number 150. Many reports showed that k_{ov} is independent from Re_{org} at any flow regime (Doig *et al.*, 1999; Boontawan, 2005). This is due to the high diffusivity of solute in the organic solvent. As a result, the

system can be operated at low Re_{org} just to ensure the homogeneous condition in the organic phase in order to reduce the operation cost. Finally, product in the organic phase was recovered by simple distillation, and the organic solvent was reused.

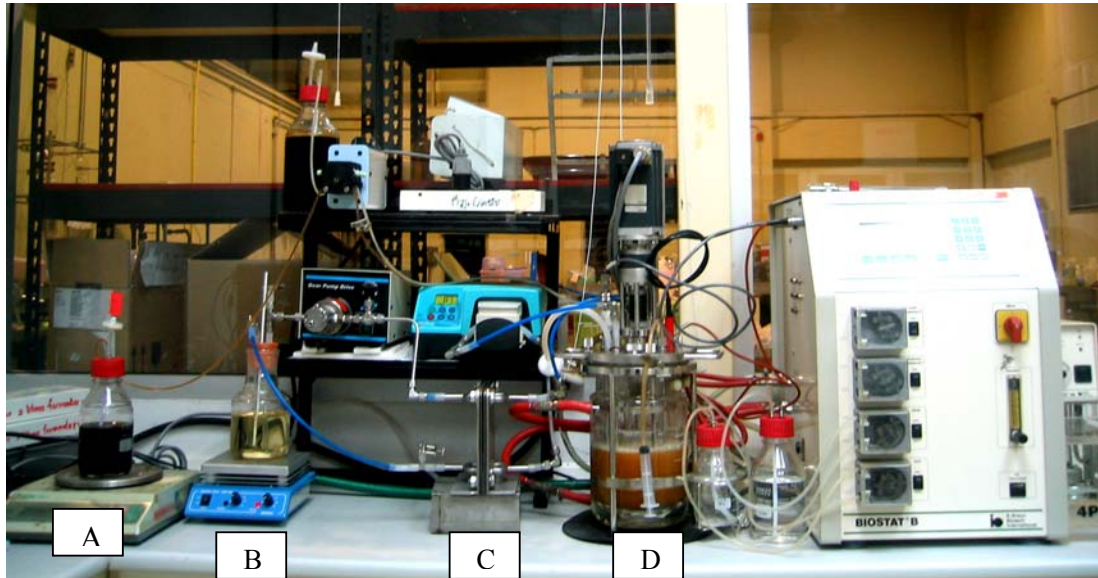


Figure 10 Membrane bioreactor set up for fed-batch fermentation of ethanol by perstraction technique. A is the molasses, B is the organic solvent, C is the membrane module, and D is the bioreactor.

2.6 Analysis

2.6.1 Quantitative analysis of ethanol

Ethanol concentrations in both organic and liquid phase were determined using capillary gas chromatography (PerkinElmer AutosystemXL, USA). 3 μ L of sample was injected into a 30 m PE-Wax column. Samples from organic phase were injected directly, whilst the aqueous phase samples were extracted with 1-decanol prior to inject into the GC. The injection port and detector temperature was both set at 250 °C. The temperature profile was set as follows; initial temperature was set at 70 °C and was held for 1 minute

before increasing the temperature at 20 °C /min up to 250 °C, and then held for 3 minutes. Quantitative analysis was performed by direct comparison with the integrated peak area of the calibration curve of the standard ethanol.

2.6.2 Biomass concentrations

Determination of cell concentration was carried out using spectrophotometer at 600 nm wavelength. Samples were taken, and centrifuged at 6000×g for 2 minutes. Supernatants were discarded, and the pellets were re-suspended with distilled water. The samples were diluted if necessary, and the absorbance was converted to cell concentration by a standard calibration curve of Dry Cell Weight (DCW) (Dhinakar, 1996).

$$C_x = 0.42 \times OD_{600} \quad (34)$$

The calibration curve was accomplished by filtering 3 mL of various concentrations of suspended biomass through a pre-weighed and pre-dried 0.2 µm filter paper (Whatman, UK). Deionised water was used to wash the filter, and the biomass residue was dried at 105 °C for 24 hr. The error in the biomass concentration measurement was ± 5% at a concentration of 1 g.L⁻¹ based on the standard deviation of 3 independent measurements of the samples.

2.6.3 Sugar concentrations

Estimation of residual glucose concentration in the fermentation broth was carried out using phenol-sulfuric method by measuring the optical density (absorbance) of a

sample using a spectrophotometer at 490 nm. Total sugar concentrations were analyzed by phenol–sulfuric acid method using sucrose as a standard (Dubios *et al.*, 1956).

2.6.4 Microscopy

Total cell concentration by Direct Microscopic Method (Total cell count) in order to counting the both viable cell and death cell. The fermentation broth was periodically removed from the bioreactor for analysis of the number of living cells by Direct Microscopic Method (Total cell count). This method starts from pipette 1.0 ml of the sample into a tube containing 1.0 ml of the dye methylene blue which attach only to the dead cells. The mixture was subsequently filled into the chamber of a haemocytometer counting chamber before placing a cover slip over the chamber, and focus on the squares using 400X (40X objective). Finally, count the number of living cell in 5 large double-lined squares. For those organisms on the lines, count those on the left and upper lines but not those on the right and lower lines. Divide this total number by 5 to find the average number of living cell per large square (Gary, 2005).

CHATER III

Results and Discussions

3.1 Membrane Characterization

3.1.1 Preparation of PDMS and composite PDMS/PVDF membrane

The initial characterization of the membranes was performed using scanning electron microscope (SEM). This analysis provided some information on the structure and pore size of the supportive layer, allowing initial hypotheses to be made in term of the mass transfer properties. Figure 11 reveals the cross-sectional area for morphology examination on internal structure of PDMS membrane. A dense thick layer of PDMS was formed after evaporation of hexane as the organic solvent. According to information provided by Dow Corning, this type of polymer can be cross-linked under ambient condition whilst most common silicone rubbers require heat treatment to enhance the bondage between chains of the polymer. For composite PDMS/PVDF membranes, asymmetric support layers were firstly prepared by immersion-precipitation method. SEM pictures of various PVDF compositions between 10 to 20% were taken, and revealed different internal void structures (data not shown). Asymmetric membranes are layered structures in which the porosity, pore size or composition change from the top to the bottom surface of the membrane (Baker, 2004). Figure 12 shows support layer with dope composition at 15% PVDF in n-methyl pyrrolidone supplement with 4g of LiCl as non solvent additive. At this composition, the best internal structure was obtained. The

top surface possesses a thin, very finely micro-porous structure whilst the bottom layer has finger-like void structure which extends from just under the dense skin to the bottom surface. This supportive layer possesses superb internal structure with good mechanical properties, and was therefore chosen for fabrication of composite membrane.

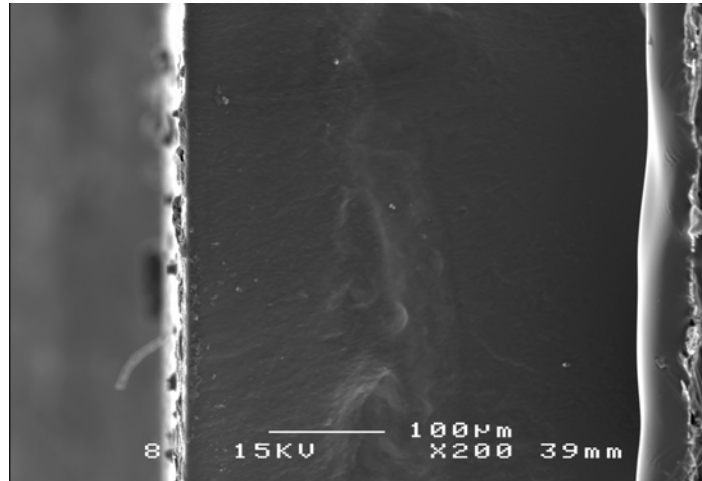


Figure 11 Scanning electron micrograph of PDMS membrane prepared by solution casting technique.

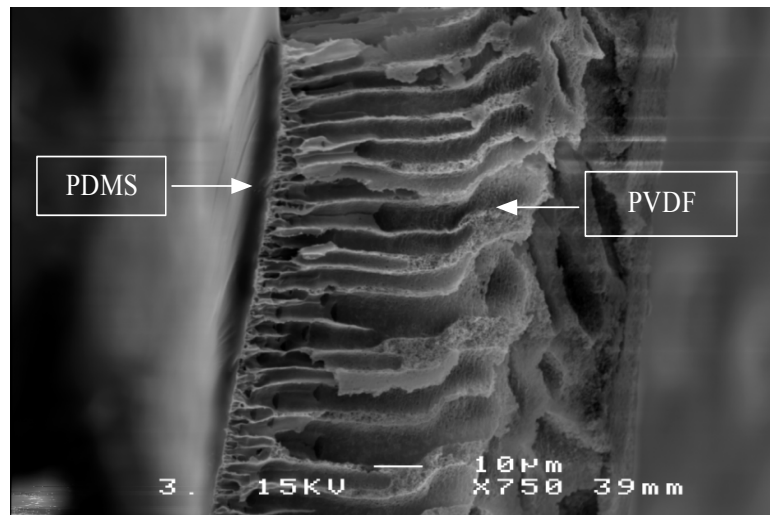


Figure 12 SEM picture of composite PDMS/PVDF support membrane casting from phase inversion technique (showed PVDF layer has finger-like)

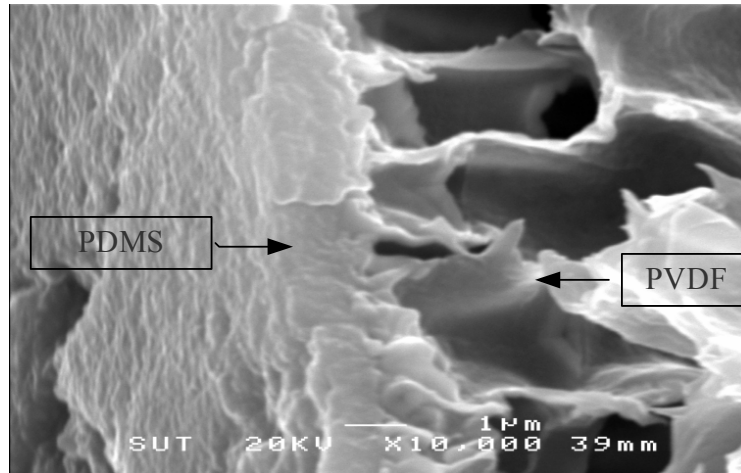


Figure 13 Scanning electron microscope picture of composite PDMS/PVDF membrane

Figure 13 shows the SEM analysis of the composite membrane with the PDMS layer uppermost, and the support PVDF layer underneath. PDMS membrane top layer is tightly and properly cast on the top of the PVDF membrane, displaying a uniform coating thickness of approximately 1-3 μm . Ideally, in the fabrication of composite membranes, it is desirable to have a minimum coating thickness with as little membrane resistance as possible (Daisley *et al.*, 2006). With the characteristic of large and finger-like pores structure, the resistance from support layer can be neglected. Comparisons of separation performances between thick and composite membrane were then carried out.

3.2 Partition coefficients

In order to gain an insight into mass transfer characteristic in liquid-liquid contacting system, determinations of partition coefficient of organic/aqueous coefficient ($P_{\text{aq}}^{\text{org}}$) and partition coefficient of membrane/aqueous ($P_{\text{aq}}^{\text{mem}}$) were carried out. Previous work (Roddy, 1981) showed the order of extraction capacity of ethanol to be hydrocarbon < ether < ketone < amine < ester < alcohol. In addition, long chain alcohols were

successfully used as extractants for organic-aqueous two phase system (Mattiasson and Holst, 1991). Hence, 2 types of alcohols; medium chain (pentanol), and long chain alcohol (1-decanol) were employed in this work for comparison of such parameters.

3.2.1 Membrane/aqueous coefficient (P_{aq}^{mem})

When silicone membranes are in contact with organic solvents, they will swell to varying degrees; this phenomenon results from the hydrophobic interaction between the organic solvent and the membrane phase. The polymer chain in the membrane then stretches to varying degrees depending on the organic solvent used (Bitter, 1991).

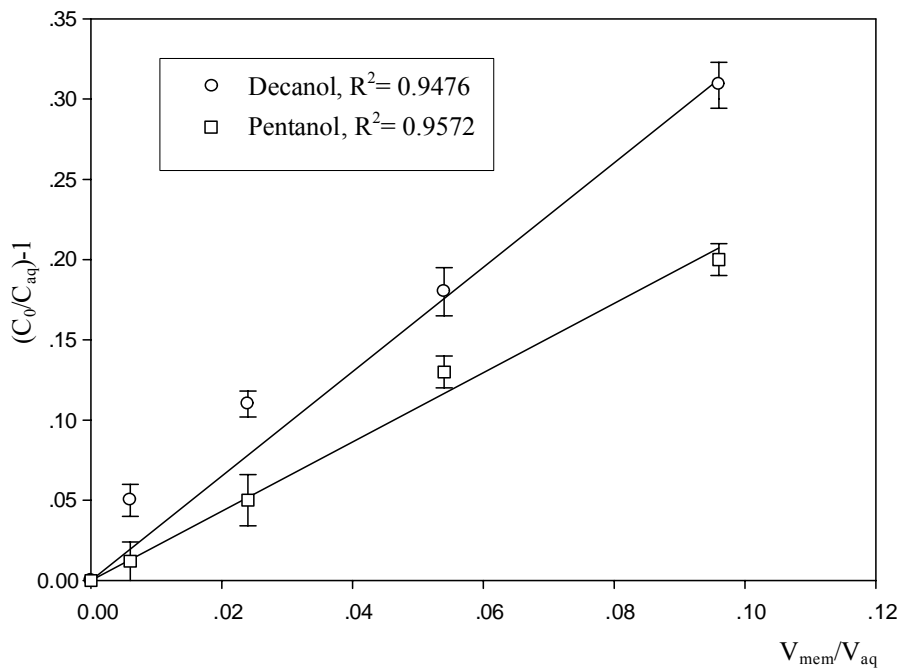


Figure 14 Equilibrium curve of ethanol partitioning into membrane immersed in pentanol, and 1-decanol at 30°C

However, both types of organic solvent did not result in membrane swelling since no volume change was observed. Figure 14 displays the graphical determination for P_{aq}^{mem} of ethanol in membrane submerged in pentanol and 1-decanol. As expected, both

data shows linear relationship between the increasing masses of membrane and the decreasing equilibrium concentrations of ethanol. The results show that ethanol partition in membrane submerged in 1-decanol more than in pentanol with the value of 3.25 and 2.15, respectively. The magnitude of P_{aq}^{mem} is quite useful to predict the mass transfer characteristic of ethanol through the membrane matrix in the perstraction system. Previous work (Doig *et al.*, 1999) classified a high P_{aq}^{mem} when the value is greater than 25 whilst a low P_{aq}^{mem} is one less than 5. The resistances-in-series model (equation 20) is the most widely used to predict the mass transfer characteristic across the membrane. For organic solutes which possess high P_{aq}^{mem} , the membrane resistance should be negligible so that different membranes thicknesses are not significantly alter the k_{ov} . Hence, the only controlling step in this particular case is the aqueous resistance (k_{aq}). In the case of our experiments, P_{aq}^{mem} values for both membranes were lower than 5, so that they were considered as low value. As a result, a suggestion can be made that one more parameter that plays a crucial role on the k_{ov} is the membrane resistance associated with membrane thickness.

3.2.2 Organic/aqueous partition coefficients (P_{aq}^{org})

Organic/aqueous partition coefficients for ethanol were obtained using pentanol and 1-decanol as organic solvents. The ethanol partition coefficient was defined as the ratio of the equilibrium concentration of ethanol in organic phase to aqueous phase.

Table 4 Determination for organic/aqueous partition coefficient of ethanol at 30 °C.

Ethanol concentration in solvent (g.L ⁻¹)		Ethanol concentration in aqueous (ethanol/water mixture), (g.L ⁻¹)	P _{aq} ^{org}
Pentanol	0.49	0.49	1.0
1-Decanol	1.05	0.01	105

Table 5 Determination for membrane /aqueous partition coefficient and organic/aqueous partition coefficient of ethanol at 30°C

Organic solvent	P _{aq} ^{mem}	P _{aq} ^{org}
Pentanol	2.15	1.0
1-Decanol	3.25	105

From the equation 12, Table 4 shows the results of extraction capacity of ethanol in both solvents. The results show that 1-decanol possess much higher partition coefficient to ethanol than pentanol. Table 5 indicated P_{aq}^{mem} and P_{aq}^{org} which P_{aq}^{mem} can be determined follow by equation 22. As a result, ethanol is more absorbed in 1-decanol; therefore, it is more suitable than pentanol, and was chosen for further experiments. In addition, water solubility of 1-decanol (20 °C) is 0.37 g.100 mL⁻¹ which is sparingly low compared to pentanol (2.7 g.100 mL⁻¹). This is because 1-decanol has longer hydrocarbon backbone, and exhibit more hydrophobicity. This feature facilitates further solvent recovery process.

3.3 Mass transfer consideration of a membrane in liquid-liquid contacting system

3.3.1 Absorption and diffusivity of ethanol in PDMS membrane.

The absorption and diffusion across the membrane (thickness 100 μm) can be considered the most important steps, whilst desorption is much less influence on the overall mass transfer consideration (Boam, 1996). Therefore, resistance in the boundary layer of the feed side, and membrane resistance are important to understand. The effect of aqueous hydrodynamics on the k_{ov} can be investigated separately, whilst the main contribution of membrane resistance arises not only from the chemical potential gradient across the membrane, but also the membrane permeability which is a product of the solubility and diffusion coefficient of the solute in the membrane (equation 23). As a result, understanding the diffusion coefficient in the membrane material is of great interest. After a piece of silicone sheet was immersed in a dilute solution of ethanol, the absorption of solute into the membrane occurred due to the interaction between the two components. Sampling was carried out periodically in order to analyze the concentration of ethanol until equilibrium was reached. The theoretical diffusivity of was then calculated by plotting the absorption characteristics in the silicone membrane sheet. A non-steady state model, as seen in Equation 9, was used to calculate the diffusivity by plotting $\ln(1 - M_t / M_\infty)$ against t , and the membrane diffusivity is obtained from the slope.

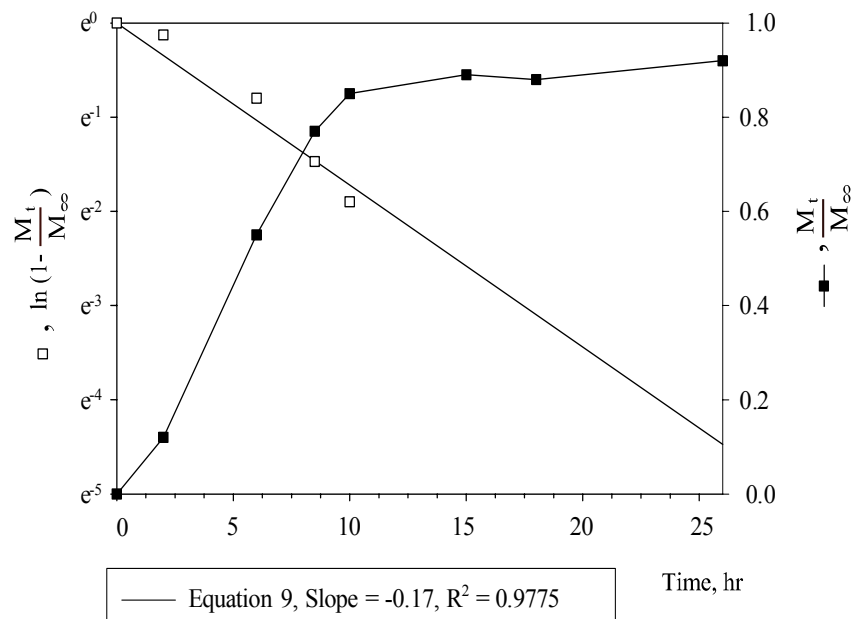


Figure 15 Absorption characteristic of ethanol in the PDMS membrane sheet, thickness 100 μm (saturated with 1-decanol) as a function of time (T=30°C)

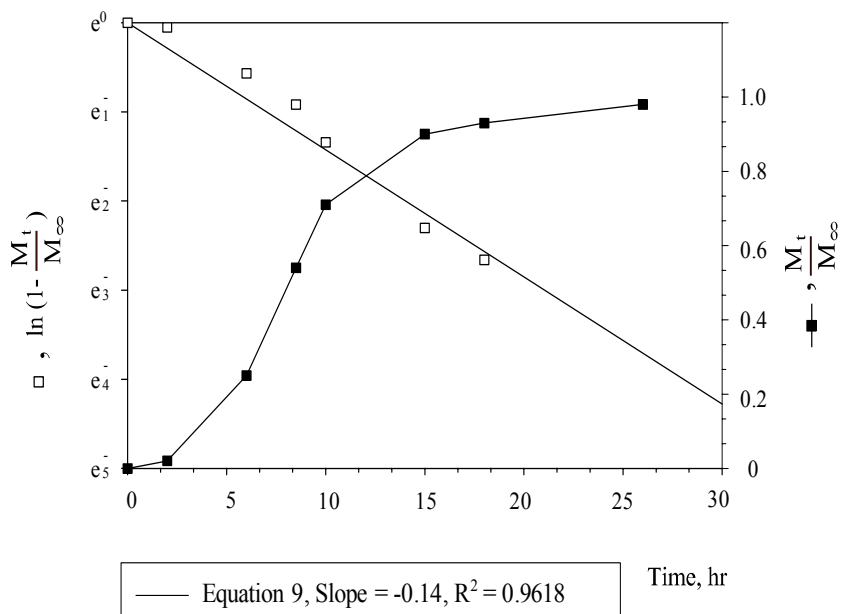


Figure 16 Absorption characteristic of ethanol in the PDMS membrane sheet, thickness 100 μm as a function of time (T=30°C)

Uptake of ethanol in the membrane matrix occurred linearly until about 10 hours before the uptake rate decreased, and equilibrium was reached after 20 to 25 hours. The experimental data before equilibrium were used to calculate the theoretical D_{mem} . A straight line can be fitted to the experimental data, and this showed a good compatibility with the equation. In this particular case, the diffusivity of ethanol in a silicone membrane saturated with 1-decanol was $2.07 \times 10^{-10} \text{ m}^2 \cdot \text{s}^{-1}$, whilst the calculated D_{mem} in membrane without saturation was $1.70 \times 10^{-10} \text{ m}^2 \cdot \text{s}^{-1}$, respectively. The latter value showed approximately the same order of magnitude with the previous work of $1.50 \times 10^{-10} \text{ m}^2 \cdot \text{s}^{-1}$ (Watson and Payne, 1990).

3.3.2 Mass transfer analysis and overall mass transfer coefficient (k_{ov})

Mass transfer for extraction of ethanol from the aqueous phase is a consequence of concentration gradient between the two liquid phases, and also to favorable partitioning into the organic phase. Therefore, the overall mass transfer coefficient (k_{ov}) can be estimated using experimental data obtained from the mass flux of ethanol through the silicone membrane based on the organic phase concentration. Typical experimental data for mass transfer characteristic of ethanol through silicone membrane in liquid-liquid contacting system were obtained as shown in Figure 17. In order to maintain the initial concentration (driving force) in the aqueous phase relatively constant throughout the extraction experiment, a large volume of aqueous phase was achieved using a 2 L glass reservoir. Initially, ethanol was absorbed into the membrane matrix from the aqueous phase resulting in a small lag phase of approximately 1 hour before a continuous and linear increase in concentration in the organic phase occurred. However at the end of the

run, mass flux of ethanol declined before eventually reached a plateau. This is because the reduction of driving force during the experiment. Figure 18 reveals a graphical determination of k_{ov} for the extraction of ethanol from the aqueous phase from the experimental data shown in Figure 17. Only linear correlation data were used to find the k_{ov} since pseudo-steady state occurred. Pseudo steady state is a condition in which it is convenient to assume steady state for portions of a non-steady state system.

As mentioned earlier, a plot of time against the RHS of equation 33 results in a straight line with the slope of k_{ov} . The experimental data fitted very well with the equation ($R^2 = 0.9765$), and the k_{ov} was obtained directly from the slope as $2.64 \times 10^{-8} \text{ m.s}^{-1}$ as shown in Figure 18.

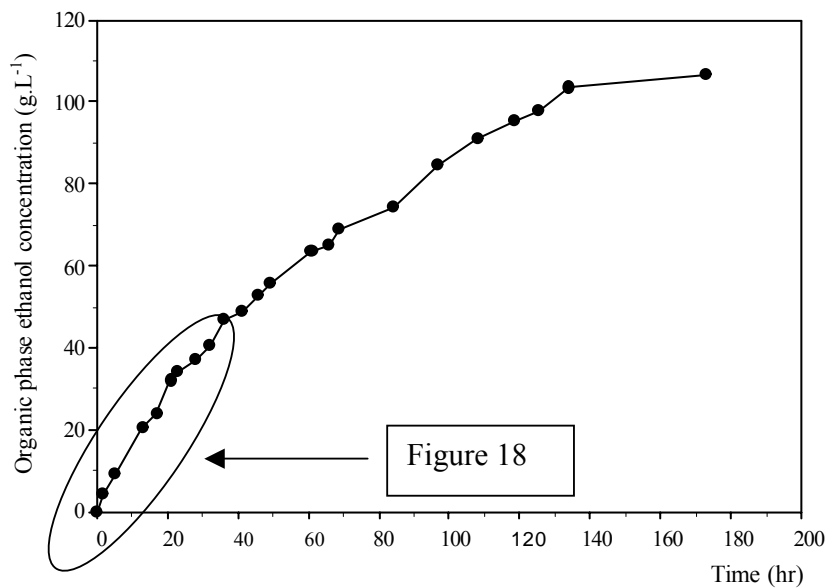


Figure 17 Time course of ethanol concentration in organic reservoir (1-decanol) during the mass transfer experiment using PDMS membrane. ($\delta = 500 \mu\text{m}$, $V_{\text{org}} = 500 \text{ mL}$, $V_{\text{aq}} = 2\text{L}$, initial ethanol concentration in aqueous phase = 10%, 30°C)

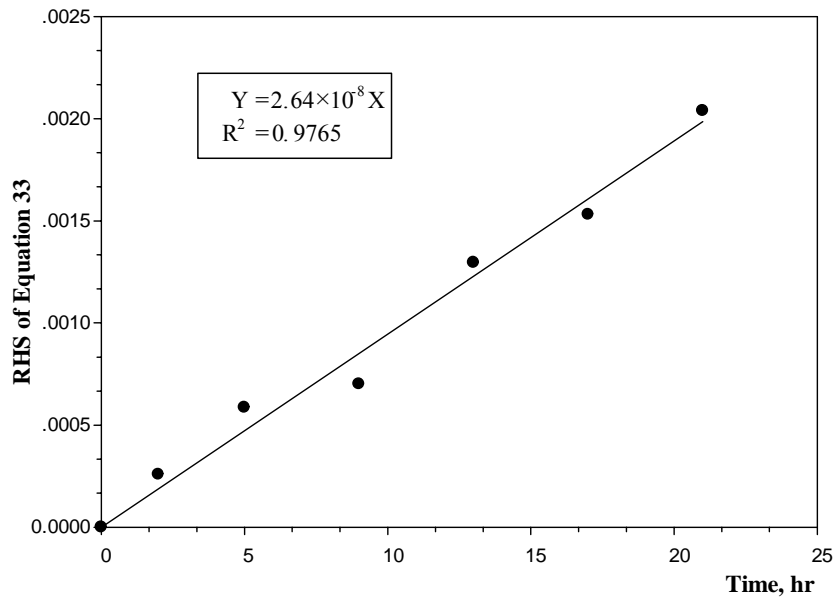


Figure 18 Graphical determination of k_{ov} for Figure 17

The resistances-in-series model is generally used to explain mass transport characteristics of the perstraction system (Wijmans and Baker, 1995). Overall mass transfer resistance is considered to be the sum of the resistances due to the aqueous boundary layer, the membrane, and the organic boundary layer. However, the organic boundary layer resistance on the permeate side is normally negligible since diffusivity of the organic solutes in organic phase is much larger than in aqueous phase (Doig *et al.*, 1999; Boontawan, 2005). Consequently, the overall mass transfer resistance at steady state condition as seen in equation 19 can be reduced as;

$$\frac{1}{k_{ov}} \approx \frac{1}{k_{aq}} + \frac{1}{k_{mem} P_{aq}^{org}} \quad 35$$

As the k_{ov} for this particular experiment was obtained under defined conditions, further investigations into the operating conditions; such as, effect of aqueous hydrodynamic condition (Re_{aq}), and membrane thicknesses will enable greater insights

into parameters which could affect the system performance. However, other operating conditions; for example, pH, and Temperature were not performed because those parameters need to set to the same optimum condition in fermentation broth. In addition, the effect of initial ethanol concentration to the mass flux was not investigated. This is because typical ethanol concentration in the broth at the end of fermentation process is always in the magnitude of approximately 10%.

3.3.3 Effect of membrane thicknesses

As mentioned earlier, membrane swells in various degrees when in contact with organic solvents, and therefore affect some operating parameters. Firstly, a high P_{aq}^{org} will reduce the organic phase boundary resistance; and secondly a high P_{aq}^{org} suggests that P_{aq}^{mem} will also be high and thus the membrane resistance should be negligible (Doig *et al.*, 1999). Accordingly, the rate limiting step is therefore the diffusion in the aqueous phase. Although organic/aqueous partition coefficient for ethanol in 1-decanol is high (105), the value of P_{aq}^{mem} is rather low (0.9). Hence; the membrane resistance (k_{mem}) also plays a major role on the overall mass transfer coefficient. For k_{mem} , the permeability of the hydrophobic molecules through the membrane phase is governed by three parameters which are P_{aq}^{mem} , membrane thickness (δ), and the membrane diffusion coefficient (D_{mem}) as followed;

$$\frac{1}{k_{mem}} = \frac{\delta}{D_{mem} P_{aq}^{mem} P_{aq}^{org}} \quad (36)$$

From the mass transfer analysis, it can be suggested that higher permeability of membrane results in the higher rate of ethanol flux. In a given operating condition, the

value of D_{mem} , $P_{\text{aq}}^{\text{mem}}$, and $P_{\text{aq}}^{\text{org}}$ are constant. Since the mass flux rate is proportional to the thickness, it should be as thin as possible in order to minimize the effect of membrane resistance. Three thicknesses of membranes were employed in this study, 300 μm , 100 μm and approximately 2 μm (composite membrane). Figure 19 shows the effect of membrane thicknesses to the overall mass transfer coefficients.

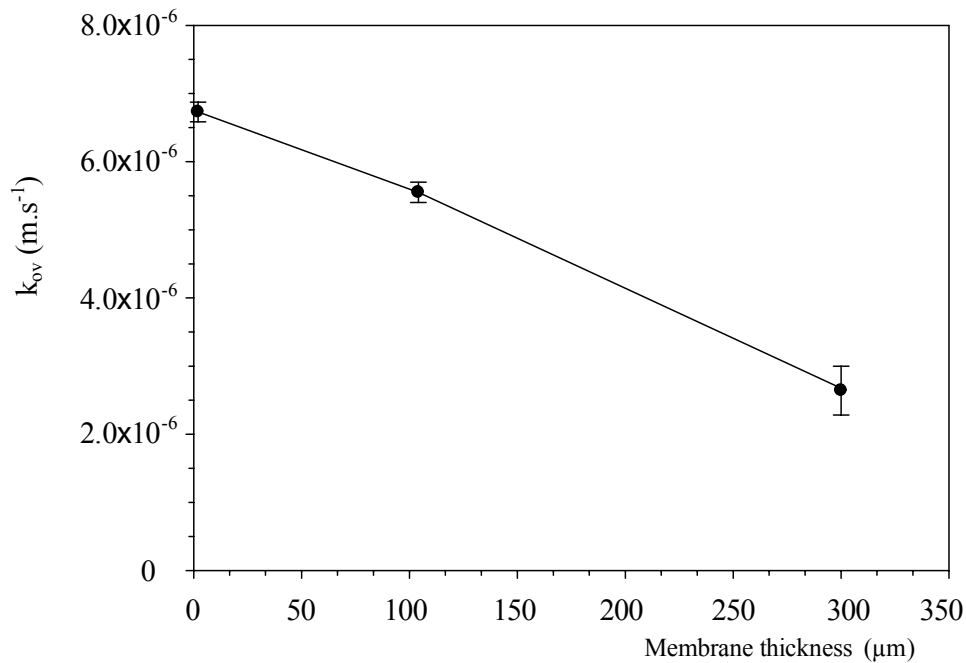


Figure 19 Effect of membrane thickness on the k_{ov} ($V_{\text{org}} = 500 \text{ mL}$, $V_{\text{aq}} = 2\text{L}$, $E^0 = 10\%$, $\text{Re}_{\text{aq}} = 4000$, $\text{Re}_{\text{org}} = 150$, 30°C).

In the system conditions, aqueous phase and organic phase Reynolds number were fixed at 4000 and 250, respectively whilst temperature was controlled at 30°C . As expected, the ethanol transfer rate through composite PDMS/PVDF membrane was higher than 100 μm PDMS and 300 μm PDMS. The magnitudes of k_{ov} were obtained with the range of 2.6×10^{-6} to $6.8 \times 10^{-6} \text{ m.s}^{-1}$, respectively. As a result, it can be concluded that the thickness of membrane have profound effect on mass transfer coefficient. Thus, this study successfully produced an extremely thin layer membrane which provides high

k_{ov} for ethanol extraction, and the fabricated membrane was employed to study *in situ* ethanol removal from fermentation broth in a membrane bioreactor.

3.3.4 Effect of aqueous Reynolds numbers (Re_{aq})

The influence of aqueous hydrodynamic effect to the perstraction performance was shown in Figure 20. Transition from laminar to turbulent flow depends not only on the velocity of the fluid, but also on its viscosity, density and the geometry of the flow conduit. A parameter used to characterize fluid flow is the Reynolds number. The boundary layer grows in thickness from the leading edge until it develops on the Reynolds number for bulk flow (Doran, 1995). The effect of liquid phase hydrodynamics was quantified and compared via the influence they had on the overall mass transfer coefficient. The aqueous flow rate was varied in the range of 0.42-1.20 L.min⁻¹, and the corresponding Reynolds number was estimated to be approximately 1400-4000. The feed flow regimes on the aqueous side of the membrane surface were therefore transition and turbulent (Reynolds number ≥ 4000).

The magnitude of overall mass transfer coefficients were obtained in the range of 3.46×10^{-7} to 4.21×10^{-6} m.s⁻¹. Experimental data revealed that the aqueous phase hydrodynamics have a profound effect on mass transfer. As the aqueous Reynolds numbers increased, the values of k_{ov} increased. This phenomenon confirms the existence of theoretical aqueous film resistance.

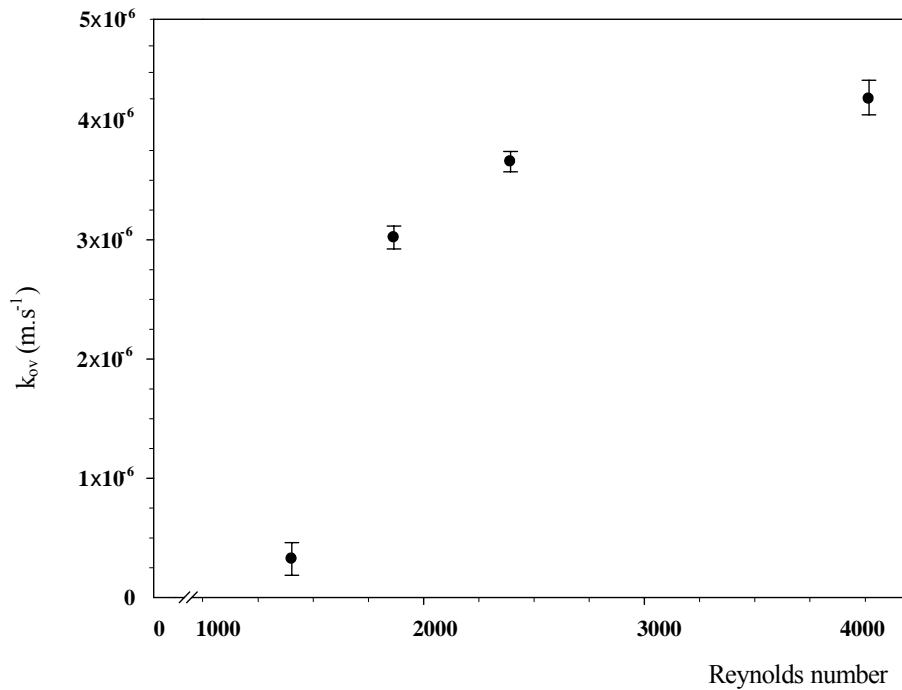


Figure 20 Effect of aqueous phase Re on k_{ov} for the extraction of ethanol from aqueous phase to 1-decanol. ($Re_{org} = 250$, composite membrane).

An explanation for this is that under the low flow regime in the laminar region, mass transfer from the aqueous phase to the membrane occurs only by diffusion through the boundary layer, whilst for the higher flow regime, mass transfer occurs by both diffusion and convection due to the formation of eddies in the aqueous phase directly contacting the membrane surface. The thickness of theoretical aqueous boundary layer is then reduced. In addition, the boundary layer effect at a given membrane thickness becomes more significant at lower Reynolds numbers.

3.4 Fermentation kinetics

3.4.1 Effect of initial cell concentrations

The purpose of this study was to gain an insight into the effect of biomass concentration on the volumetric production rate of ethanol, and productivity in batch mode. The resulting biomass obtained from the batch fermentation was centrifuged, and was subsequently re-suspended into different concentrations (5-25 g.L⁻¹) before addition of the molasses. Experiments were carried out in rotary shake flasks and the system performances were then monitored.

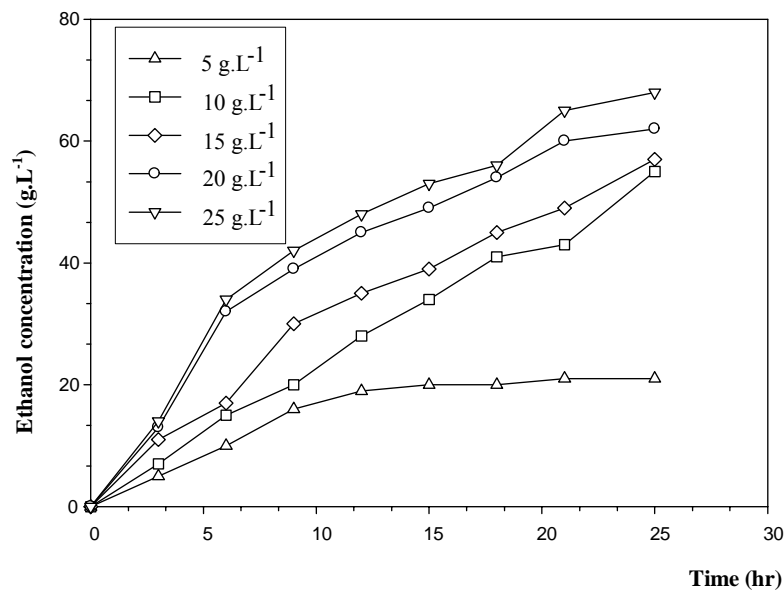


Figure 21 Time course concentration of ethanol with different initial cell concentrations. (Initial total sugar concentration 125 g.L⁻¹, T = 30 °C and 250 rpm).

Time courses for evolution of ethanol from sugar cane molasses by *S. cerevisiae* in batch fermentation are shown in Figure 21. All set of experimental data showed a linear relationship at the beginning of the process followed by a declined production rate toward the end of the process. The production of ethanol ceased at the end of the fermentation process, and it was clearly due to inhibition effect of ethanol to the

biocatalyst. Production rates were obtained at the rate of 1.90, 2.46, 3.35, 5.32 and 6.14 $\text{g.L}^{-1}.\text{hr}^{-1}$ for biomass concentrations at 5, 10, 15, 20 and 25 g.L^{-1} , respectively (Figure 22). As a result, a conclusion can be made that higher biomass concentration results in higher volumetric productivity. However, most of the experiments resulted in final ethanol concentration of approximately 50-60 g.L^{-1} except $\approx 20 \text{ g.L}^{-1}$ for biomass concentration of 5 g.L^{-1} . The inhibition of this magnitude presents a potential problem in the simultaneous fermentation, presently a norm of the process scheme in ethanol production from biomass (Wu and Lee, 1997). There are advantages of process in high biomass concentration which it's could be reduced contamination from bacterial or microorganisms. Therefore, in during fermentation, systems have been shown to be useful in some circumstances as maintaining high biomass.

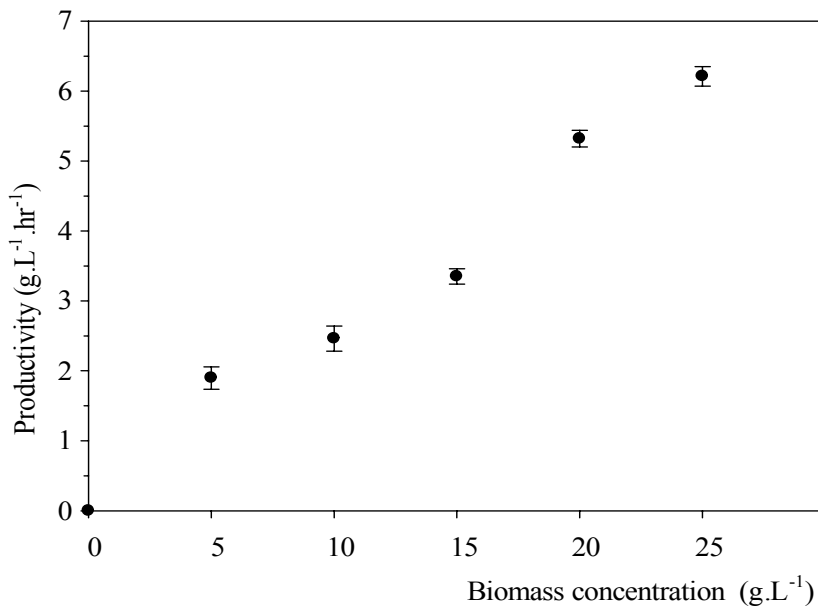


Figure 22 Effect of biomass concentration on the volumetric productivity (Initial total sugar concentration 125 g.L^{-1} , $T = 30 \text{ }^{\circ}\text{C}$ and 250 rpm).

As a result, this process was obtained the high growth rate under anaerobic conditions that is characteristic of *S. cerevisiae* an increasing ethanol concentration (Banat *et al.*, 1998). Therefore, application of high biomass concentration coupling with fed-batch process could dramatically increase both volumetric productivity and yield of ethanol. In the next section, high-cell-density cultivation was attempted and fermentation performances in fed-batch mode were investigated.

3.4.2 High cell density cultivation

In fermentation processes, there are two possible ways to enhance the volumetric productivity of the system. Firstly, increase the ethanol production rate, and secondly, reduce the toxicity using extractive fermentation or high cell cultivation. Hence, developments of upstream processing in ethanol production by *S. cerevisiae* from molasses were carried out in order to increase volumetric productivity. In addition, application of high biomass concentration could prevent inhibition effect from both substrate and ethanol to the yeast cell (Converti *et al.*, 2003). Firstly, inoculate the *S. cerevisiae* grown overnight into a special formulated YM medium in a bioreactor.

Figure 23 shows the results of high-cell-density cultivation grown in a special formulation of YM medium. The biomass concentrations increased after the inoculation with a short lag phase of approximately of 5 hours. Exponential increase in the volumetric cell concentration was observed for approximately 7 hours during the growth. The estimated specific growth rate (μ) was approximately 0.42 h^{-1} , and biomass concentration reached a constant value of approximately 25 g.L^{-1} after depletion of glucose at 22 hours. Although no others method for high-cell-density cultivation was not investigated, this simple technique satisfactorily provided a good result. In addition,

advantages can be notified including simplicity of the process and controlling procedures. The biomass obtained from this experiment was used in subsequent fermentation experiments.

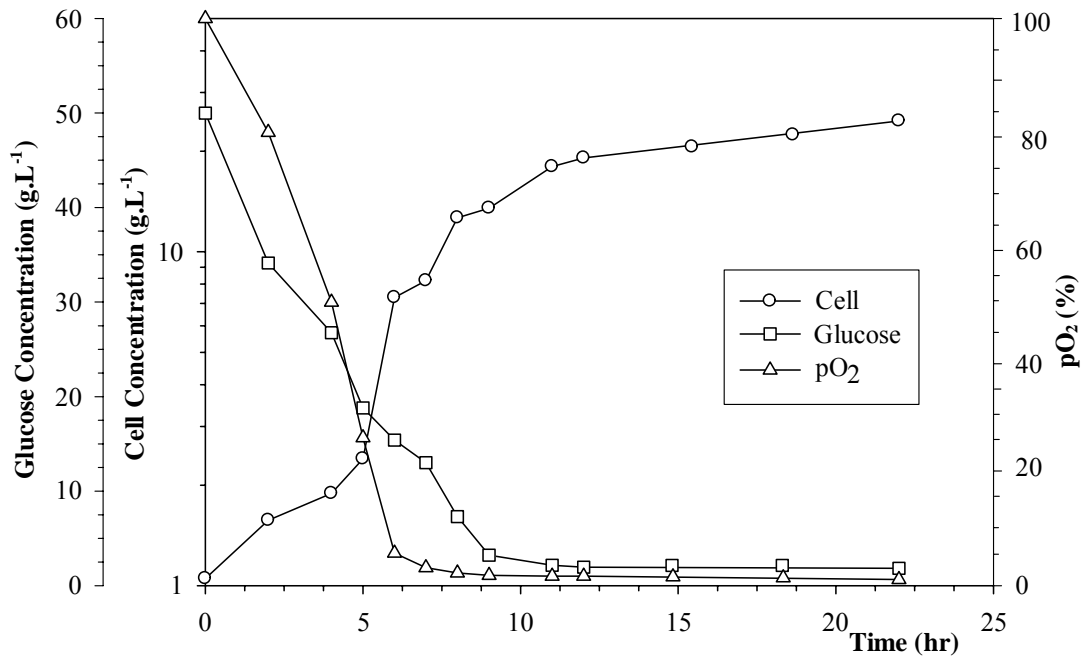


Figure 23 High biomass cultivation of *S. cerevisiae* in 3X YM medium (pH = 5.5, T = 30 °C).

3.4.3 Effect of molasses feeding rate

Fermentation of ethanol in batch process usually results in a low production yield possibly due to high inhibition of substrate and product to the yeast cells. In order to solve the problem, this experiment introduced a fed-batch process coupling with high biomass concentration. A peristaltic pump was employed to add molasses continuously to the fermentation broth after the growth ceased. Aeration was then stopped in order to create anaerobic condition. Constant feeding rate (a time parameter feeding rate constant, $K = 0$) was chosen in this work since exponentially decreasing or increasing flow rate ($K < 0$ or $K > 0$) result in non-linear productivity according to (equation 1). The molasses

was pumped into the bioreactor at constant feeding rates ranging from $0.004 \text{ g}\cdot\text{s}^{-1}$ to $0.02 \text{ g}\cdot\text{s}^{-1}$, and the system performances were then monitored. Figure 24 reveals the effect of molasses feeding rates to the system performances of the fed-batch process. During the experiments, volume of fermentation broth increased but measurements of the final volume gave only proximate values. Initial volume of the fermentation broth was combined with the volume of the molasses estimated from its mass being pumped into the bioreactor (density of molasses is $1.45 \text{ g}\cdot\text{mL}^{-1}$). Initial ethanol productivities for molasses feeding rate of $0.004 \text{ g}\cdot\text{s}^{-1}$, $0.006 \text{ g}\cdot\text{s}^{-1}$, $0.01 \text{ g}\cdot\text{s}^{-1}$ and $0.02 \text{ g}\cdot\text{s}^{-1}$ were increased with the magnitude of 2.39, 4.83, 3.65 and $3.31 \text{ g}\cdot\text{L}^{-1}\cdot\text{hr}^{-1}$, respectively.

The lowest ethanol concentration was obtained at feeding rate $0.004 \text{ g}\cdot\text{s}^{-1}$ with the magnitude of about $130 \text{ g}\cdot\text{L}^{-1}$. Production rate of ethanol was also the lowest compared to the other two rates. This was clearly due to low feeding rate of molasses, and it was not chosen for subsequent experiment. The maximum ethanol concentration ($171 \text{ g}\cdot\text{L}^{-1}$) was achieved at molasses feeding rate of $0.006 \text{ g}\cdot\text{s}^{-1}$ with the final volume of fermentation broth (V_f) at approximately 1.40 L. The total amount of ethanol obtained from this experiment is the product of ethanol concentration and the final volume ($171 \text{ g}\cdot\text{L}^{-1}\times 1.4 \text{ L}$) resulting in the value of 240 g.

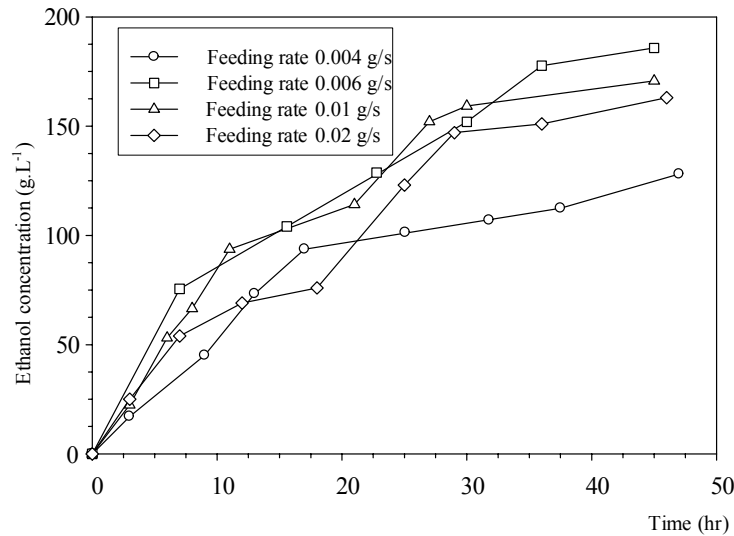


Figure 24 Effect of feeding rates on performances of molasses fermentation by *S. cerevisiae* in fed-batch process ($T = 30\text{ }^{\circ}\text{C}$, $\text{pH} = 5.5$, $V_0 = 0.75\text{ L}$).

Compared with the batch experiment (section 3.4.1, biomass concentration 20 g.L^{-1}), this amount of ethanol is almost 4 times higher than the maximum ethanol concentration obtained. This successful outcome was clearly due to massive amount of molasses supplied to the system. In addition, inhibitions associated with high initial molasses concentration were also minimized. Nevertheless, ethanol production reached a plateau at the end of fermentation process. The reason for this is clearly due to high amount of ethanol accumulated in the system leading to inhibition effect. At the feeding rate of 0.01 g.s^{-1} and 0.02 g.s^{-1} , the system performance was lower than the feeding rate of 0.006 g.s^{-1} for both initial production rate and final product concentrations (Figure 25). The reason was unclear but probably because of excessive addition of molasses.

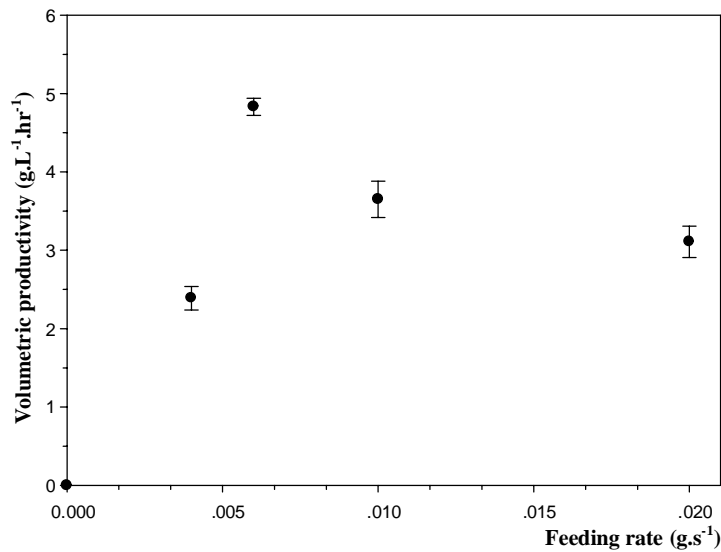


Figure 25 Effect of molasses feeding rate on the volumetric productivity.

This causes mass transfer limitations in the system and might subsequently inhibit the biocatalyst activity. So that, molasses feeding rate of 0.006 g.s^{-1} is the most suitable in subsequent experiment for *in situ* ethanol removal in a membrane bioreactor.

3.5 Membrane bioreactor setup for *in situ* ethanol removal in fed-batch fermentation

Membrane bioreactor for biotransformation/fermentation has attracted considerable interest over the last 5 years. It combines a biochemical reaction with selective mass transport of the products from the reaction site. Since the product concentration can be kept low in the bioreactor, the reaction equilibrium can be shifted forward resulting in an increase in the product yield (Giorno and Drioli, 2000). This *in situ* product removal technique makes this type of membrane reactor particularly attractive because it is simple to operate, and ideal for product inhibited reactions. As indicated in the previous section, fed-batch process has problems due to product

inhibition in the fermentation broth. Removal of ethanol from the system could therefore increase volumetric productivity and production yields. First of all, calculation of the required surface area is necessary for a given operating condition. The mass transfer rate of ethanol transferred into the organic reservoir can be given as the following equation,

$$-N_i = k_{ov} A \Delta C \quad (37)$$

In order to make the system not in the mass transfer limited, ethanol production rate should be in a magnitude of lower than the mass flux of ethanol across the membrane. If the production rate is higher, ethanol will accumulate in the fermentation broth, and could result in inhibition effect. For the application in a membrane bioreactor, mass transfer rate of ethanol (N_i) across the membrane was estimated from fermentations in Section 3.4.3. At the feeding rate of 0.06 g.s^{-1} , production rate of ethanol at $4.83 \text{ g.L}^{-1}\text{hr}^{-1}$ was obtained. Initial volume of the fermentation broth was 0.75 L , so that the volumetric productivity of ethanol in this case was 3.62 g.hr^{-1} or $1.01 \times 10^{-3} \text{ g.s}^{-1}$. Therefore, this value can be used as N_i . The k_{ov} of composite PDMS/PVDF was chosen at $6.8 \times 10^{-6} \text{ m.s}^{-1}$, and the value was obtained from section 3.3.3 operated with $Re_{aq} 4000$ and $Re_{org} 250$. Finally, the concentration gradient (ΔC) was chosen with the magnitude of 30 g.L^{-1} ($30,000 \text{ g.m}^3$). At this concentration, the yeast cells should not be affected by the ethanol. By substitution of these values into the above equation, the required membrane area can then be estimated at the magnitude of 49.5 cm^2 base on $1,000 \text{ mL}$ of organic phase. Therefore, the membrane area of this module used in this work (100 cm^2) is suitable for the application in a membrane bioreactor at the given operating condition.

3.5.1 Operation of membrane bioreactor for *in situ* ethanol removal in fed-batch fermentation system

In previous sections, separation of ethanol from aqueous solution in abiotic system was successfully investigated. In addition, fed-batch fermentation systems coupling with high-cell-density cultivation were also studied. In this section, *in situ* separation of ethanol from fermentation broth in a membrane bioreactor was investigated. The main purpose of this experiment is to investigate the implementation of perstraction technique in order to enhance the fermentation performances including volumetric productivity and yield. The aqueous phase volume of 0.75 L and organic phase volume of 1.0 L were the starting system condition. Bioreactor was monitored, and regulated at the temperature 30 °C using an external electric control unit. Since, however, initial biomass also affects growth, the higher ethanol concentrations attained at higher biomass concentration (Alexander *et al.*, 1989). High biomass concentration of approximately 25 g.L⁻¹ from the high-cell-density cultivations was employed in this experiment, and 1-decanol was re-circulated at the other side of the membrane. Ethanol in the fermentation broth was then extracted through the membrane, and was collected in the organic reservoir. Figure 26 shows the performance of the *in situ* ethanol removal in a membrane bioreactor using perstraction technique. The graph was plotted using average values of triplicate set of experimental data. At the beginning, organic ethanol concentration gradually increased during the first 5 hours due to the absorption into the membrane matrix and low driving force at the beginning of the biotransformation processes.

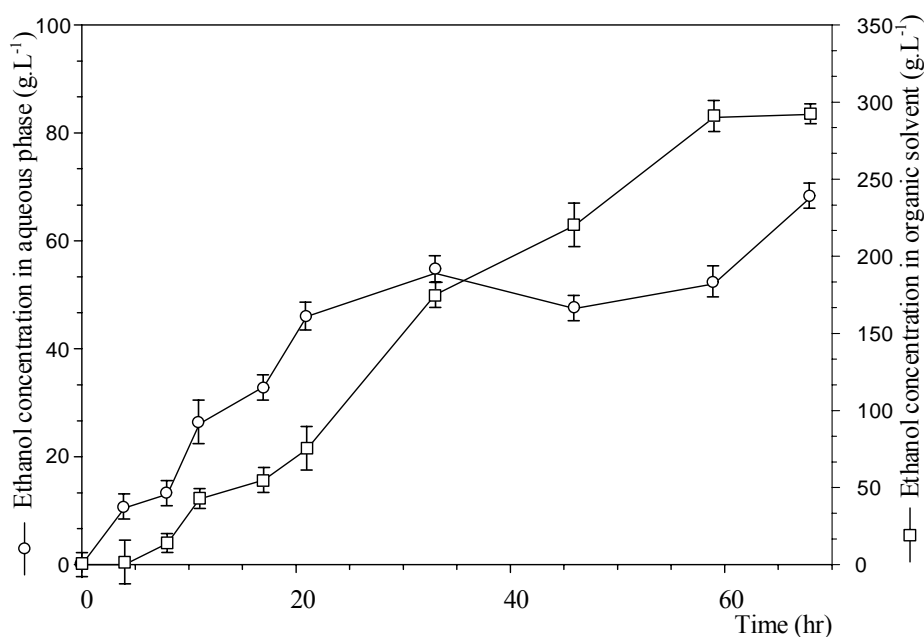


Figure 26 Organic phase and aqueous phase (bioreactor) concentration of ethanol during fed-batch fermentation in a membrane bioreactor.

The ethanol concentration then increased linearly indicating that the system was successfully operated. The highest ethanol obtained from this system was nearly 300 g.L⁻¹, and aqueous ethanol concentration was maintained at about 50 g.L⁻¹ before reaching 75 g.L⁻¹ at the end of the process. Compared with fed-batch fermentation, this work clearly showed improved ethanol productivity, and minimized the effect of product toxicity to the yeast cells by instant removal of ethanol into the organic reservoir. In addition, the system was operated in a more stable and longer periods of time. Improvement of mass flux was obtained with a constant ethanol production rate of 4.73 g.L⁻¹hr⁻¹ throughout fermentation time before the biochemical reaction stopped at over 60 hours. Compared to approximately 40 hours of fed-batch process, this long period of ethanol production rate is clearly resulted from low product inhibition to the yeast cells. Production yield ($Y_{P/X}$)

in the membrane bioreactor was an order of magnitude higher than fed-batch fermentation (12.0 versus 9.6 $\text{g}_{\text{Ethanol}} \cdot \text{g}^{-1}_{\text{Cell}}$). Removing the ethanol during fermentation increases the yield by allowing more to be produced from a given amount of biomass, plus increases the production rate by reducing the accumulation of an inhibitory product (Hahn and Alex, 2003). Throughout the run, the yeast cells were retained in the bioreactor and continuously produced ethanol without significant deactivation.

Nevertheless, this membrane bioreactor was able to be operated for quite a short period of time which is lower than expectation. Despite the instant product removal, the consequence for this phenomenon is unclear but probably from by product of fermentation by the yeast and/or yeast to die (metabolically shutdown) at high glucose concentrations used in fermentation (Scott, 2004). In addition, this inhibition problem probably due to nutrient limitation or toxin accumulation in the broth, mechanism stress also contributes to cell deactivation (Chimica, 2006). On the other hand, membrane fouling by cell debris is also improbable. PDMS membranes have non-porous structure that is not clogged by cell or cell debris. Therefore, this membrane will be very useful in producing low-molecular weight compounds or ethanol. As a result, problems associated with fouling effect can be neglected. Since the toxicity of molasses to the yeast cells is beyond the scope of this work, further experiment on toxicity effect was not carried out.

3.5.2 Investigation for the system stability

It is generally accepted that accumulation of ethanol in the fermentation broth results in cell death. Previous chapter investigated *in situ* ethanol removal, and found that higher production yield was obtained comparing to the fed-batch system. In order to confirm the consequence, quantitative analysis of the cell viability measurement by direct

microscopic counting method was chosen because this technique is simple and reliable. This method distinguishes between viable cells and death cells by staining the yeast cells with methylene blue before examining them under microscope. Only death cells will be positively stained with the dye. Samples were taken periodically, and cell viability was assessed by counting the ratio of death to living cells under the microscope. The number of viable cells (C_x) were compared with the number of viable cell at the beginning of the run (C_x^0) and the ratio was subsequently used to calculate the deactivation constant (k_d) as follows;

$$\frac{C_x}{C_x^0} = e^{-k_d t}$$

Take natural logarithmic on both sides of the equation gives

$$\ln \frac{C_x}{C_x^0} = -k_d t$$

A plot of $\ln C_x / C_x^0$ against time (hours) results in a straight line, and the deactivation constant (k_d) can be estimated directly from the slope. In addition, the half-life of the biocatalyst can then be calculated as;

$$t_{1/2} = \frac{\ln 2}{k_d}$$

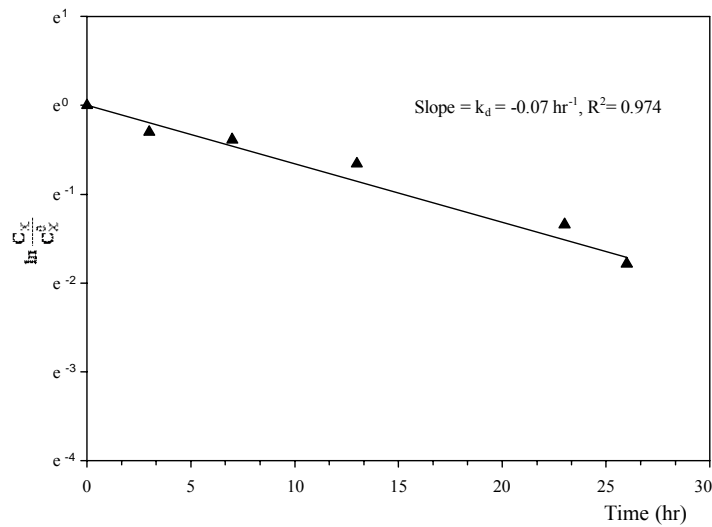


Figure 27 Deactivation constant study in batch fermentation ($T = 30\text{ }^{\circ}\text{C}$, $\text{pH} = 5.5$, biomass concentration = 25 g.L^{-1}).

Figure 27 illustrate the relative viability ($\ln C_x / C_x^0$) of the yeast cells during batch fermentation. Initial biomass concentration was 25 g.L^{-1} . The experimental data were plotted against time of operations, and resulting in the deactivation constant at 0.07 hr^{-1} . In batch fermentation where molasses is prepared before the inoculation, the system is subjected to high initial substrate concentration in the fermentation broth as well as all other toxic substances. The main problem for this system is the high contact between the biocatalyst, the toxic substrates, high osmotic pressure, and ethanol which could result in a short biocatalyst life-time. The estimated value of biocatalyst half-life was 9.90 hours.

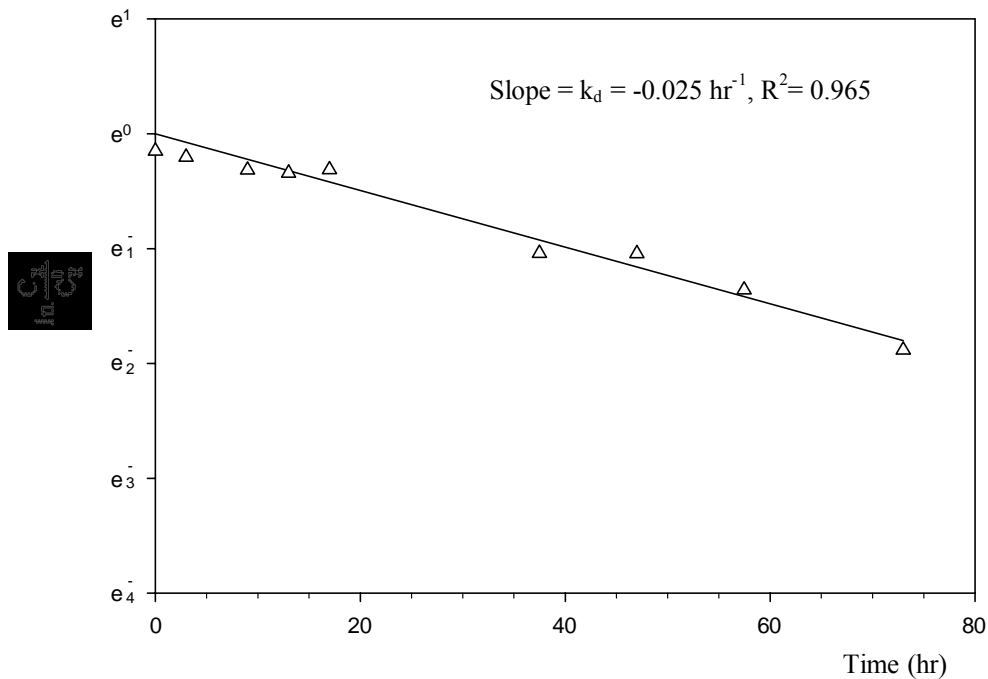


Figure 28 Deactivation constant in fed-batch fermentation (Molasses feeding rate = 0.006 g.s^{-1} , $T = 30 \text{ }^\circ\text{C}$, $\text{pH} = 5.5$, agitation speed = 250 rpm).

Figure 28 shows the investigation of deactivation constant in a fed-batch process. All operating conditions were set as same as the batch experiment except that molasses was fed separately at the rate of 0.006 g.s^{-1} . From the results, it was clear that the yeast cells were much more stable than the batch process with a deactivation constant (k_d) of 0.025 hr^{-1} . The biocatalyst half-life was calculated to be approximately 28 hours. This result of extended half-life was clearly due to minimization of deleterious effects from addition of molasses of the batch process. However, the system was still vulnerable to the accumulating toxic substances especially the ethanol in the fermentation broth.

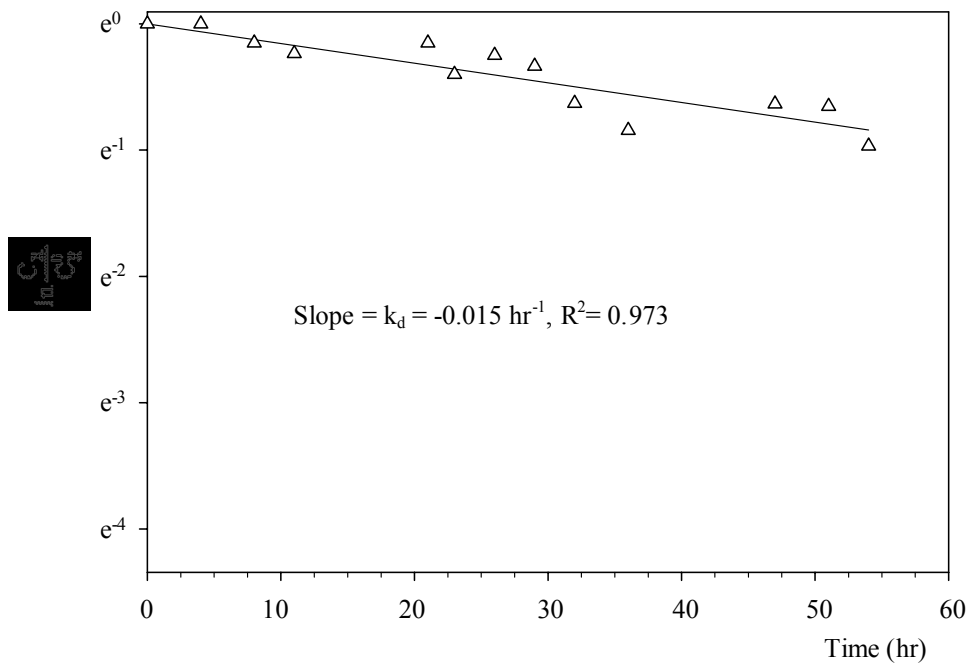


Figure 29 Deactivation constant of *S. cerevisiae* in fed-batch fermentation with *in situ* ethanol removal in a membrane bioreactor.

Figure 29 reveals the relative viability of *S. cerevisiae* over time during the fed-batch fermentation with *in situ* ethanol removal. This technique successfully attempted to minimize the effect of product inhibition by reduce the deactivation constant to 0.015 hr^{-1} with the estimated biocatalyst half-life of approximately 46 hours. During fermentation, yeast growth is rapidly stopped when the concentration of alcohol in the medium increases but fermentive activity is not entirely inhibited until high alcohol concentrations are reached. The rate of alcohol accumulation within the cells and certain kinetic parameters were simultaneously determined in such fermentative processes using yeast cells (Navarro and Durand, 1978). This process demonstrated that the problems associated with product inhibition can be minimized resulting in a reduced death rate. Because ethanol concentration in the fermentation broth was kept low, this results in

higher final concentration, and production yield. As a result, the application of this system could consequently enhance economic viability for commercial production. Despite attempts on the reduction of substrate and product toxicity effect, the experimental result revealed only approximately 40% of deactivation constant lower than fed-batch fermentation. The experimental result was not as expected, and the reason for this was unclear. However, further investigation of such effect to the yeast cells is beyond the scope of this study.

CHAPTER IV

CONCLUSIONS AND RECOMMENDATIONS

The whole thesis was divided into five parts including membrane characterization, partition coefficients, mass transfer study, fermentation kinetic and membrane bioreactor for *in situ* ethanol removal in fed-batch fermentation. For the fermentation of ethanol, the strain of *S. cerevisiae* used in this work is a good ethanol producer. On the other hand, economic constraints make the large scale production of this low cost product depended on cheap sources of carbon and nitrogen such as molasses from the sugar industry. However, the conventional processes have problems especially product inhibition from ethanol accumulated in the systems. Thus, this work attempted on application of membrane in liquid-liquid contacting system to separate ethanol from the fermentation broth. High mass transfer rate through the membrane can be accomplished by either increase the membrane surface area or reduce the membrane thickness. This work produced the membrane which possesses extremely thin membrane as composite PDMS/PVDF membrane for an application in perstraction system. Selective layer of polydimethylsiloxane (PDMS) with the thickness of $\approx 1-5 \mu\text{m}$ was successfully coated on a polyvinylidene fluoride (PVDF) membrane support in order to form composite PDMS/PVDF membrane. It is clear that membrane thickness is inversely proportional to the k_{ov} . This composite membrane demonstrated refined perstraction techniques compared with the other or traditional membranes that had only one thick active

permselective layer. Effect of aqueous hydrodynamics were also investigated, and proved the existence of theoretical boundary layer. In addition, perstraction technique offers advantages over conventional product recovery processes, particularly in term of preventing emulsion formation from the organic-aqueous two phase system. The product-rich organic phase obtained can then be easily further purified by conventional separation processes. In addition, subsequent reuse of the organic phase is then possible. As a result, this work successfully established a thorough understanding of ethanol mass transfer characteristic including absorption and diffusion behavior through the non-porous PDMS membrane. Fermentation kinetics in fed-batch process were investigated, and showed that high ethanol concentration accumulated in the broth result in severe inhibition effect. Therefore, proposed process for *in situ* ethanol removal using composite PDMS/PVDF membrane separation was suggested. Since ethanol was continuously removed from the fermentation broths through the membrane, the effect of product inhibition was minimized. This work expands the range of application of the membrane bioreactor for biotransformation/fermentation. The experimental results indicated that this work is a modest improvement in ethanol fermentation in term of increasing volumetric productivity and production yield, and ease of ethanol recovery from the system. Hence, it is useful to further investigate this *in situ* product removal technique in pilot-scale, and this could lead to implement this system in an industrial scale production. However, in order to be a viable technology on a large scale, this membrane module need to be scaled-up by several orders of magnitude to several 100 or 1,000 m² for high mass transfer rate and to supply the biocatalyst with sufficient reactant. Finally, many problems still remain particularly inhibition from molasses, and high required membrane surface

area which should be solved to make the perstraction technique more practically attractive.

4.1 Further Research Works

4.1.1 Pretreatment of molasses or usage of more suitable carbon source

This thesis used molasses as substrate for ethanol fermentation which is a good raw material because of its low cost and readily available. However, molasses is still contain inhibitors which are unfriendly to the microorganisms (Roukas, 1995), for example, metal ions and high sugar concentration, and especially anti-fungal compounds which may be added in order to preserve the molasses. As a result, pretreatment of molasses is encourage; for example, ion-exchange for removal of heavy ions. In addition, further work can be investigated using more suitable raw materials especially hydrolyzed tapioca starch. There are many results for choosing this raw material; firstly, it contains no inhibitors when cooked; secondly, it is cheap (≈ 2 Baht/kg); and finally, it is readily available in Nakhonratchasima province.

4.1.2 Improve the design of membrane module

Our membrane module employed in this work has limitations especially low membrane area which is not suitable for high rate of ethanol extraction. This is because it possesses low membrane area per unit volume of the bioreactor. Furthermore, scale up the processes could encounter problems, especially in the design of the membrane module. However, a new proposed design for the membrane module which gives both high membrane area and low membrane resistance is strongly recommended. Moreover,

fabrication of a relatively thin membrane as well as a novel membrane module design could enhance the economic aspect of the membrane bioreactor for ethanol recovery in fed-batch process.

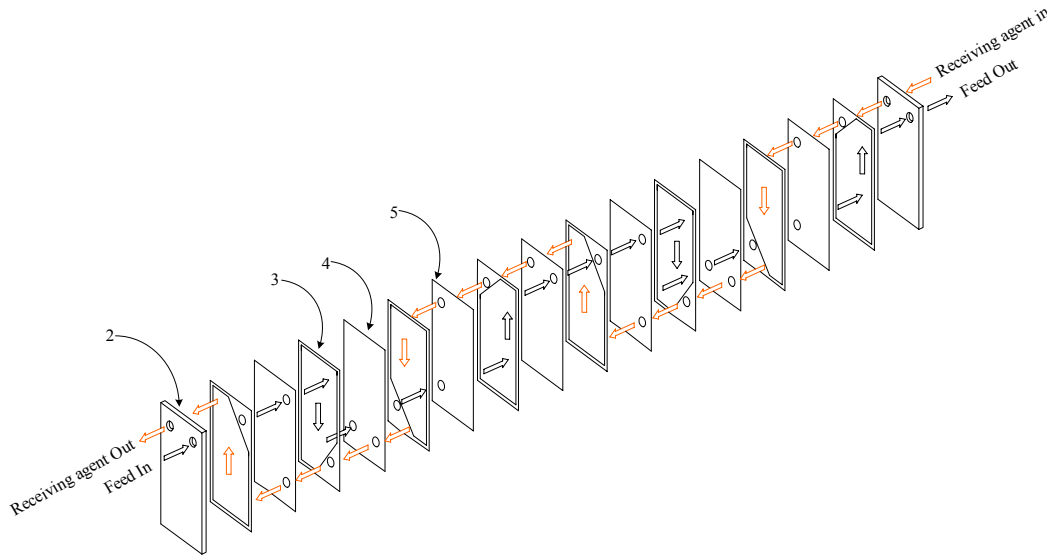


Figure 30 Schematic diagram of the plate-and-frame mass exchanger.

Figure 30 details the working principle of a newly design membrane module. It somehow resembles plate-and-frame heat exchanger except that the plates are replaced by the flat sheet membranes (no 4, 5). The membranes are situated between gaskets (no.3) which provide flow channels and housed in between a pair of stainless steel frames (no. 2). The aqueous feed stream can be pumped in one side of the frame whilst the receiving solution can be circulated from the other end. The two liquid phases then flow inside the module on the opposite direction. The main advantage of this module is that the mass transfer area can be increased as much as possible by increasing the number of the flat sheet membrane. Figure 31 shows an experimental setup for a membrane bioreactor for *in situ* ethanol removal from the fermentation broth. The membrane module (A) can be seen in the middle-left of the figure. Unfortunately, this membrane module was not functioned

properly due to some leakage of water between the gaskets. As a result, experimental data could not be obtained.

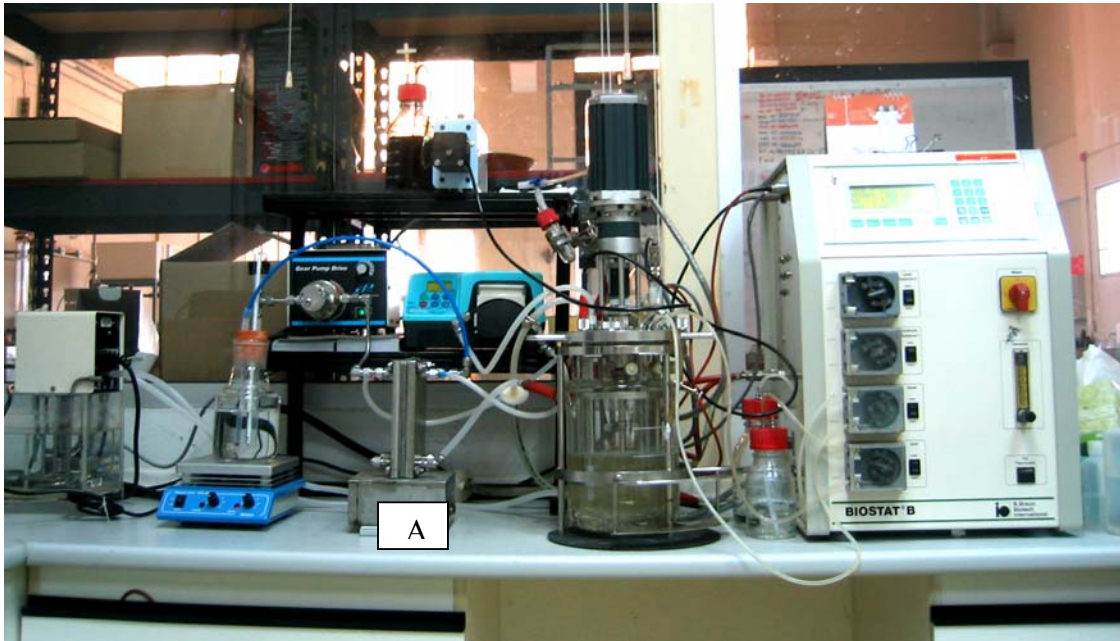


Figure 31 An experimental setup for a flat sheet membrane bioreactor for *in situ* removal of ethanol from fermentation broth, A is the membrane module.

4.1.3 Protection against ethanol toxicity

Although ethanol concentration in the fermentation broth was kept low ($\approx 50 \text{ g.L}^{-1}$), the biocatalyst could still be subject to inhibitory effect of the highly toxic product. Therefore development of some of protection methods against ethanol toxicity would be essential to make up a much efficient extractive fermentation system (Matsumura and Kmarkl, 1984). Numerous efforts could be introduced, and investigate for the system performance; for example, immobilized cell could be developed using adsorbents which possess a strong affinity to the solvent such as sodium alginate. The adsorbent trapped the toxic molecules coming into the gel beads, and reduced the solvent concentration in the gel beads to much less than that in the fermentation broth. The

protector in gel beads is effective until it is saturated with solvent. Durability of the protective effect depends on the amount of protector in gel beads, and on the concentration of ethanol in the fermentation broth (Mattiasson and Holst, 1991).

REFERENCES

REFERENCES

(Thairath, 2548).

http://www.thairath.co.th/thairath1/2548/column/scooper/sep/12_9_48.php.

Alexander, M. A., T. W. Chapman and T. W. Jeffries (1989). Continuous-Culture Responses of *Candida shehatae* to shifts in Temperature and Aeration: Implications of Ethanol Inhibition, Vol. 55, pp. 2152-2154.

Ann, V. S. (2000). Extractive fermentation of ethanol production, M.Sc. thesis, Queen's university, Canada.

Bailey, J. and O. Ollis (1986). *Biochemical Engineering Fundamentals*, McGraw-Hill, New York.

Baker, R. W. (2004). *Membrane technology and applications*, John Wiley & Sons, England.

Banat, I. M., P. Nigam, D. Singh, R. Marchant and A. P. McHale (1998). Ethanol production at elevated temperatures and alcohol concentrations: Part I - Yeasts in general, *World Journal of Microbiology and Biotechnology*, Vol. 14, pp. 809-821.

Beavan, M. J., C. Charpentier, C. Rose and A.H. (1982). Production and tolerance of ethanol in relation to phospholipids fatty acryl composition in *Saccharomyces cerevisiae* NCYC 431, *Gen Microbiol*, Vol. 128, pp. 1447-1455.

Bitter, J. G. A. (1991). *Transport mechanisms in membrane separation processes*, Plenum press, London.

Boam, A. (1996). Novel bioreactor design for the biotransformation of hydrophobic compounds, Ph.D. thesis, University of London.

Boontawan, A. (2005). A membrane bioreactor for biotransformation of terpenes, Ph.D. Thesis, Imperial College London.

- Cartwright, C. P., J. R. Juroszek, M. J. Beavan, M. S. Ruby, S. M. F. Morais and A. H. Rose (1986). Ethanol dissipates the proton-motive force across the plasma membrane of *Saccharomyces cerevisiae*, *Gen Microbiol*, Vol. 132, pp. 369-377.
- Carvalho, J. C. M., E. Aquarone, S. Sato, M. L. Brazzach, K. A. Almeida and W. Borzani (1993). Fed-batch alcoholic fermentations of sugar cane blackstrap molasses: influence of the feeding rate on yeasts yield and productivity, *Appl Microbiol Biotechnol*, Vol. 38, pp. 596-598.
- Casey, G. P. and W. M. Ingledew (1986). Ethanol tolerance in yeasts, *Crit Rev Microbiol*, Vol. 13, pp. 219-290.
- Caylak, B. and F. V. Sukan (1998). Comparison of Different Production Processes for Bioethanol, *Chemistry*, Vol. 22, pp. 351-359.
- Chimica, O. (2006). A microbiological perspective on renewable energy sources, in *Chemistry Today*, vol. 24, pp. 21pp. 21-25.
- Converti, A., S. Arni, S. Sato, J. C. M. de Carvalho and E. Aquarone (2003). Simplified modeling of fed-batch alcohol fermentation of sugarcane blackstrap molasses, *Biotechnol Bioeng*, Vol. 84, pp. 88-95.
- Crank, J. (1979). *The Mathematics of Diffusion*, Clarendon Press, Oxford, UK.
- Cussler, E. L. (1997). *Diffusion; Mass Transfer in fluid systems*, Cambridge university press.
- Daisley, G. R., M. G. Dastgir, F. C. Ferreira, L. G. Peeva and A. G. Livingston (2006). Application of thin film composite membranes to the membrane aromatic recovery system, *J Membr Sci*, Vol. 268, pp. 20-36.
- database, e. c. (2006). MEMBRANE SEPARATION PROCESS FOR DEHYDRATING A GAS OR VAPOUR OR LIQUID MIXTURE BY PERVAPORATION, VAPOUR PERMEATION OR GAS SEPARATION, in, vol., European Patent Office.

- de Pinho, M. N., R. Rautenbech and C. Herion (1990). Mass transfer in radiation grafted pervaporation membranes, *J Membr Sci*, Vol. 54, pp. 131-143.
- Dhinakar, K. (1996). Lab Exercise 2: Yeast Fermentation, University of Colorado-Boulder, Chemical Engineering Dept.
- Di, S. M., T. R. and E. Satacesaria (2001). A kinetic and mass transfer model to simulate the growth of baker's yeast in industrial bioreactors, *Chem Eng J*, Vol., pp. 377-389.
- Doig, S. D. (1998). Development of a dense phase membrane bioreactor for the biotransformations of hydrophobic molecules, Ph.D. thesis, Imperial College London.
- Doig, S. D., A. T. Boam, D. I. Leak, A. G. Livingston and D. C. Stuckey (1998). A Membrane Bioreactor for Biotransformation of Hydrophobic Molecules, *Biotechnol Bioeng*, Vol. 58, pp. 587-594.
- Doig, S. D., A. T. Boam, A. G. Livingston and D. C. Stuckey (1999). Mass transfer of hydrophobic solutes in solvent swollen silicone rubber membranes, *J Membr Sci*, Vol. 154, pp. 127-140.
- Dombek, K. M. and L. O. Ingram (1985). Determination of intracellular concentration of ethanol in *Saccharomyces cerevisiae* during fermentation, *Appl Environ Microbiol*, Vol. 51, pp. 197-200.
- Doran, P. M. (1995). *Bioprocess Engineering Principles*, Academic Press, London.
- Dubios, M., K. A. Gilles, J. K. Hamilton, P. A. Rebers and F. Smith (1956). Colorimetric method for determination of sugars and related substances, *Anal Chem*, Vol. 28, pp. 350-356.
- Echegaray, O. F., J. C. M. Carvalho, A. N. R. Fernandes, S. Sato, E. Aquarone and M. Vitolo (2000). Fed-batch culture of *Saccharomyces cerevisiae* in sugar-cane

- blackstrap molasses: invertase activity of intact cells in ethanol fermentation, *Biomass and Bioenergy*, Vol. 19, pp. 39-50.
- Gary, E. K. (2005). Factor effecting the enumeration of microorganisms, *Appl microbiol*, Vol. 98, pp. 1354-1380.
- Giorno, L. and E. Drioli (2000). Biocatalytic membrane reactors: applications and perspectives, *Trends Biotechnol*, Vol. 18, pp. 339-349.
- Hahn, J. J. and P. Alex (2003). Fermentation GOES LARGE SCALE, Process solutions, Technology development center.
- Ho, W. and K. K. Sirka (1992). *Membrane handbook*, Vannostrand Reinhold, New York.
- Hofmeyr, J. H. S. (1997). Anaerobic energy metabolism in yeast as a supply-demand system, in *New Beer In an Old Bottle: Eduard Buchner and the Growth of Biochemical Knowledge*, Vol. 1, edited by A. C. Bowden, pp. 22pp. 225-242, Universitat de Valencia, Spain.
- Huang, R. Y. M. e. (1991). *Pervaporation Membrane Separation Process*, Elsevier, USA.
- Jaisana, P., S. Vasigarat and T. Kongleaur (2000). Single cell protein production from molasses, Khon Kaen University.
- Jiratananon, R., A. Chanachai and R. Y. M. Huang (2002). Pervaporation dehydration of ethanol-water mixtures with chitosan/hydroxyethylcellulose (CS/HEC) composite membranes II. Analysis of mass transport, *J Membr Sci*, Vol. 199, pp. 211-222.
- Kong, J. F. and K. Li (2001). Preparation of microporous PVDF hollow fibre membranes via immersion precipitation, *J Appl Polym Sci*, Vol. 81, pp. 1643-1653.
- Krauter, M., E. , S. S. Aquarone, L. J. Perego and W. Borzani (1987). Influence of linearly decreasing feeding rates on fed-batch ethanol fermentation of sugar cane blackstrap molasses, *Biotechnol lett*, Vol. 9, pp. 647-650.

- Leon, R., P. Fernandes, H. M. Pinheiro and J. M. S. Cabral (1998). Whole-cell biocatalysis in organic media, *Enzyme Microb Technol*, Vol. 23, pp. 483-500.
- Li, J., C. Chen, W. Jiang and S. Zhu (2000). A study on removal of low concentration of water from C6 solvent by pervaporation, *J membr Sci Technol*, Vol. 20, pp. 15-18.
- Livingston, A. G. (1994). Extractive Membrane Bioreactor: A new process technology for detoxifying chemical industry wastewater, *J Chem Tech Biotech*, Vol. 60, pp. 117-124.
- Lye, G. J. and J. M. Woodley (1999). Application of *in situ* product-removal techniques to biocatalytic process, *Trends Biotechnol*, Vol. 17, pp. 395-402.
- Matsumura, M. and H. Kmarkl (1984). Application of solvent extraction to ethanol fermentation, *Appl. Microbiol. Biotechnol*, Vol. 20, pp. 371-377.
- Matsuura, T. (1994). *Synthetic Membrane and Membrane Separation processes*, CRC Press, Florida.
- Mattiasson, B. and O. Holst (1991). *Extractive Bioconversions*, Marcel Dekker, New York.
- McGhe, J. E., G. S. Julian and R. W. Detroy (1982). Continuous and static fermentation of glucose to ethanol by immobilized *Saccharomyces cerevisiae* cells of different ages., *Appl Environ Microbiol*, Vol. 44, pp. 19-22.
- Mubeccel, E. and S. F. Mutlu (1999). Application of a statistical technique to the production of ethanol from sugar beet molasses by *Saccharomyces cerevisiae*, Dept. of Chemical Engineering, Gazi University, Turkey.
- Najafpour, G. D. and J. K. Lim (2002). Evaluation and Isolation of Ethanol Producer Strain SMP-6, paper presented at Regional Symposium on Chemical Engineering.

- Navarro, J. M. and G. Durand (1978). Alcohol fermentation: effect of temperature on ethanol accumulation within yeast cells, *Ann Microbiol (Paris)*. Vol. 2, pp. 215-224.
- Neelam, A. and S. Amarjit (1991). Ethanol production by thermotolerant yeast and its UV resistant mutants., *Acta Microbiol Pol.*, Vol. 40, pp. 171-175.
- Nielsen, J. and J. Villadsen (2003). *Bioreaction Engineering Principles*, Kluwer Academic, New York.
- O'Brien, D. J., L. H. Roth and A. J. McAloon (1999). Ethanol production by continuous fermentation-pervaporation: a preliminary economics analysis, *J Membr Sci*, Vol. 166, pp. 105-111.
- O'Brien, D. J., G. E. Senske, M. J. Kurantz and J. J. Craig (2004). Ethanol recovery from corn fiber hydrolysate fermentations by pervaporation., *Bioresour Technol.*, Vol. 92, pp. 15-19.
- Pauline, M. D. (1995). *Bioprocess Engineering Principles (Mass transfer)*, Academic Press Limited, San Diego, USA.
- Ranulfo, M. A., R. Mauricio and J. Ins (2003). Ethanol fermentation of a diluted molasses medium by *Saccharomyces cerevisiae* immobilized on chrysotile, *Braz. arch. biol. technol*, Vol. 46, pp.
- Roddy, J. W. (1981). Distribution of ethanol-water mixtures to organic liquid, *Ind. Eng. Chem.*, Vol. 20, pp. 104-108.
- Roukas, T. (1995). Ethanol Production form Non-sterilized Beet Molasses by free and immobilized *Saccharomyces cerevisiae* Cells Using Fed-batch Culture, *Journal of food engineering*, Vol. 27, pp. 87-96.
- Roukas, T. (1996). Ethanol Production from Non-sterilized Beet Molasses by Free and Immobilized *Saccharomyces cerevisiae* Cells Using Fed-batch Culture, *Journal of Food Engineering*, Vol. 27, pp. 87-96.

- Sanches, E. N., E. M. Alhadef, R.-L. M. H. M. and N. Pereira Jr. (1996). Performance of a continuous bioreactor with immobilized yeast cells in the ethanol fermentation of molasses-stillage medium, *Biotechnol. Lett*, Vol. 18, pp. 91-94.
- Scott, K. (2004). Ethanol 101-5: Managing Stress Factors, in *Ethanol today*, vol., pp. 36pp. 36-37.
- Taylor, F., M. J. Kurantz, N. Goldberg and J. C. J. Craig (1995). Continuous fermentation and stripping of ethanol, *Biotechnol Prog*, Vol. 11, pp. 693-698.
- Van Keulen, F., C. N. Correia and M. M. R. da Fonseca (1998). Solvent selection for the biotransformation of terpenes by *Pseudomonas putida*, *J Mol Catal B*, Vol. 5, pp. 295-299.
- Voet, V. A. (1995). Glycolysis, in *The diversity of metabolism in procaryotes*, Vol. 1, University of Wisconsin-Madison.
- Wang, D., K. Li and W. K. Teo (2000). Highly permeable polyethersulfone hollow fiber gas separation membranes prepared using water as non-solvent additive, *J Membr Sci*, Vol. 176, pp. 147-158.
- Watson, J. M. and P. A. P. Payne (1990). A study of organic compound pervaporation through silicone rubber, *J Membr Sci*, Vol. 49, pp. 171-205.
- Wee, Y. J. (2004). Utilization of sugar molasses for economical L(+)-lactic acid production by batch fermentation for *Enterococcus faecalis*, *Enzyme Microb Technol*, Vol. 35, pp. 568-573.
- Wheals, A. E., L. C. Basso, D. M. G. Alves and H. V. Amorim (1999). Fuel ethanol after 25 years., *Trends in Biotechnol*, Vol. 17, pp. 482-487.
- Wijmans, J. G. and R. W. Baker (1995). The solution-diffusion model: a review, *J Membr Sci*, Vol. 107, pp. 1-21.

William, R. C. and H. S. James (2000). Effect of Dialysate-Side Mass Transfer Resistance on Small Solute Removal in Hemodialysis, *Blood purif*, Vol. 18, pp. 260-263.

Wu, Z. and Y. Y. Lee (1997). Inhibition of the enzymatic hydrolysis of cellulose by ethanol, *Biotechnology Letters*, Vol. 19, pp. 977-979.

APPENDICES

APPENDIX A

YM MEDIUM COMPOSITION

Glucose	10 g/L
Peptone	5 g/L
Malt extracts	3 g/L
Yeast extracts	3 g/L
*Agar	15-20 g/L

For the preparation of agar plate, agar was added to the solution prior to autoclaving.

APPENDIX B

STANDARD CALIBRATION CURVE

Standard calibration curve of ethanol using pentanol as organic solvent

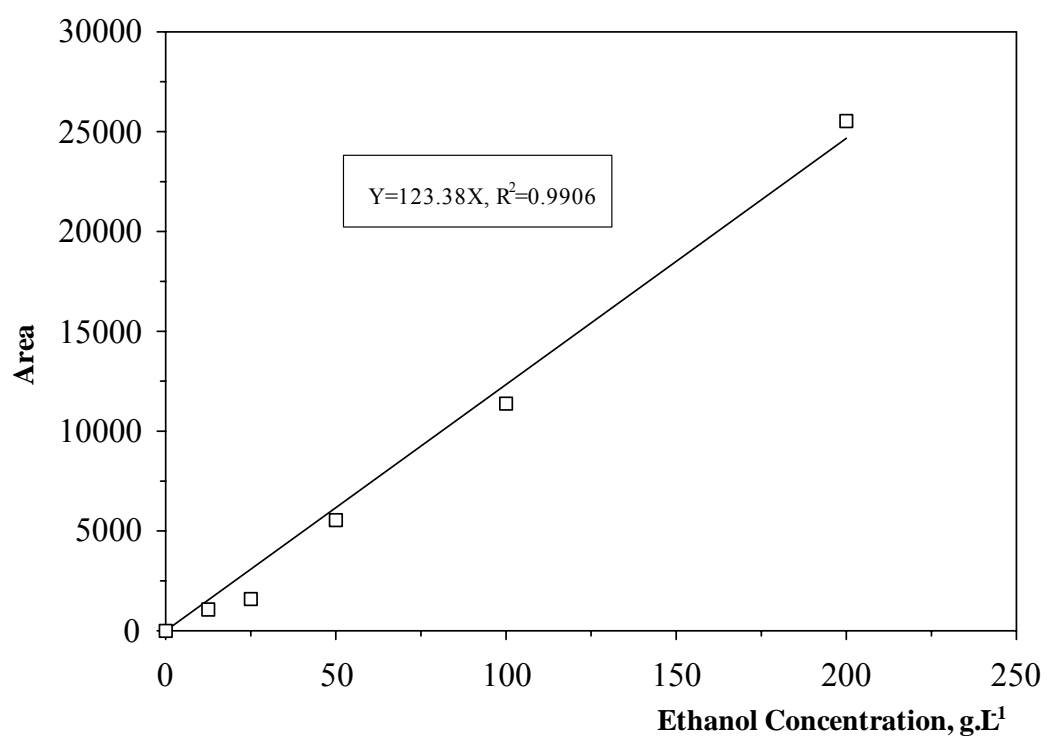


Figure 32 Standard calibration curve of ethanol using pentanol as organic solvent

Standard calibration curve of ethanol using decanol as organic solvent

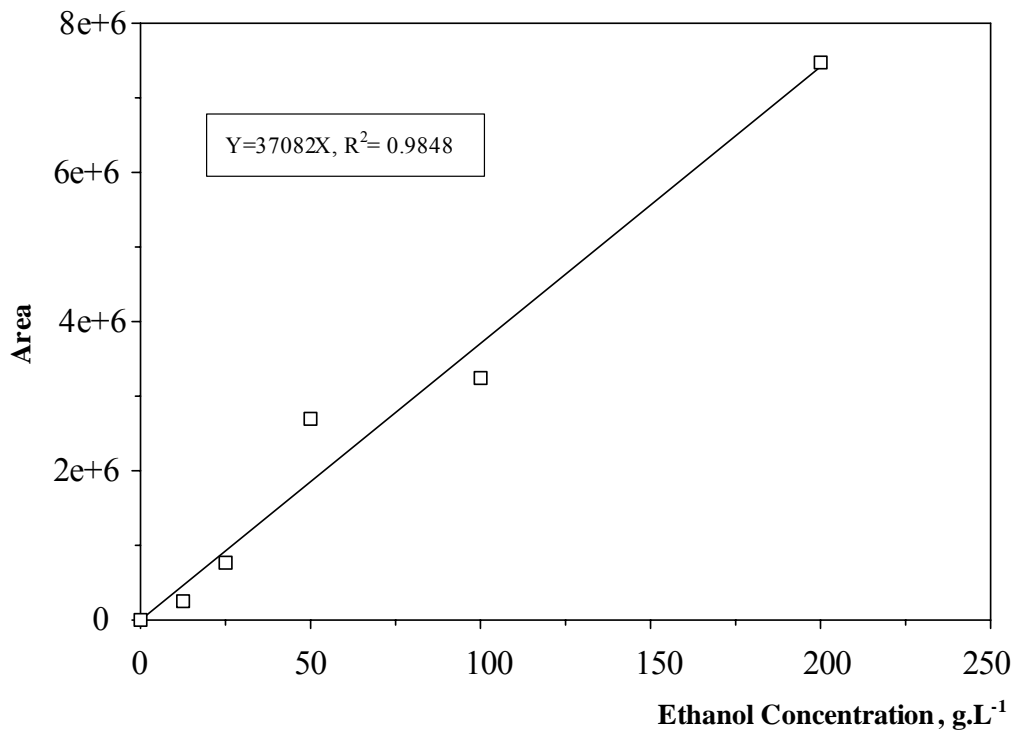


Figure 33 Standard calibration curve of ethanol using decanol as organic solvent

Standard calibration curve of cell concentration (O.D. at 600 nm)

Cell concentration by measurement density using a spectrophotometer at 600 nm and the absorbance was then converted to cell concentration by a standard calibration curve of dry cell weight.

$$C_x = 0.42 \times OD_{600}$$

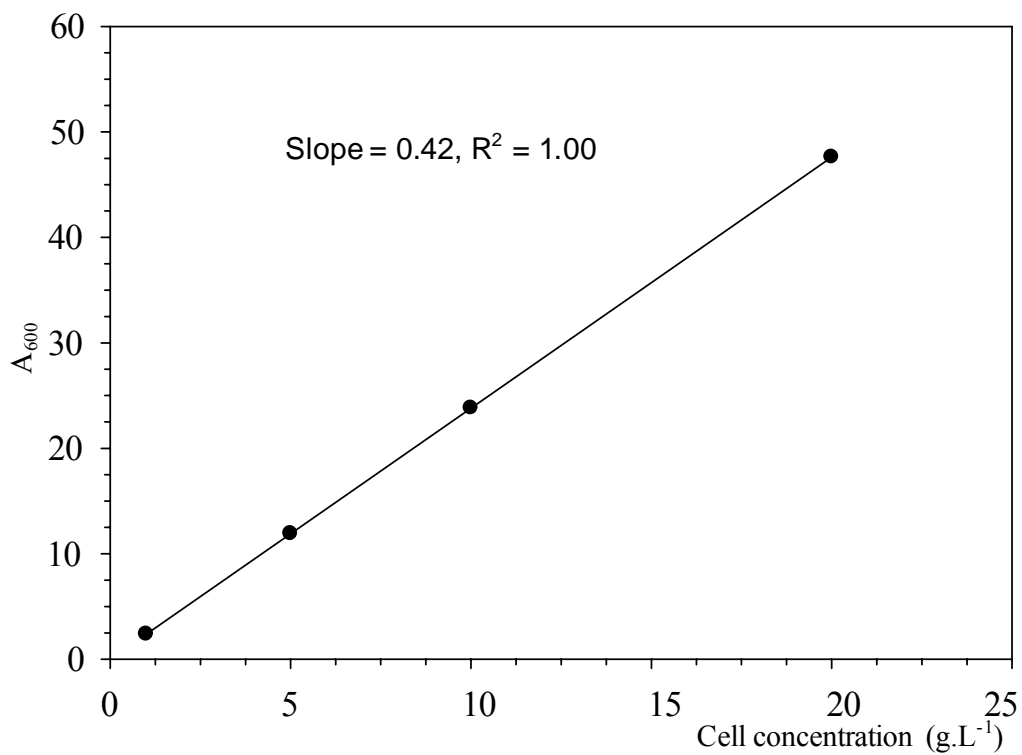


Figure 34 Standard calibration curve of cell concentration.

Standard calibration curve of sugar concentration (O.D. 490 nm)

Sugar concentration by measurement density using a spectrophotometer at 490 nm by phenol-sulfuric analysis.

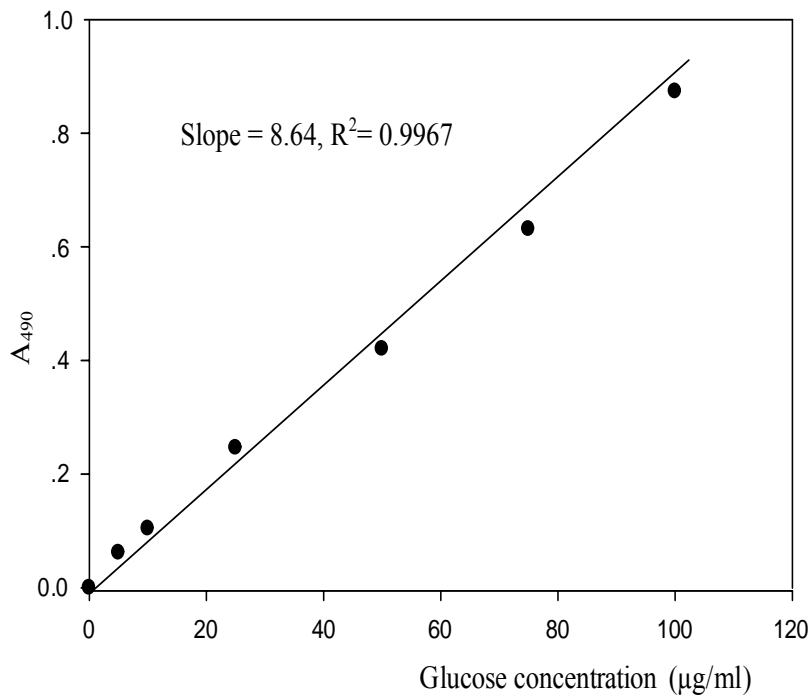


Figure 35 Standard calibration curve of sugar concentration.

APPENDIX C

Time course of glucose concentrations at molasses feeding rate

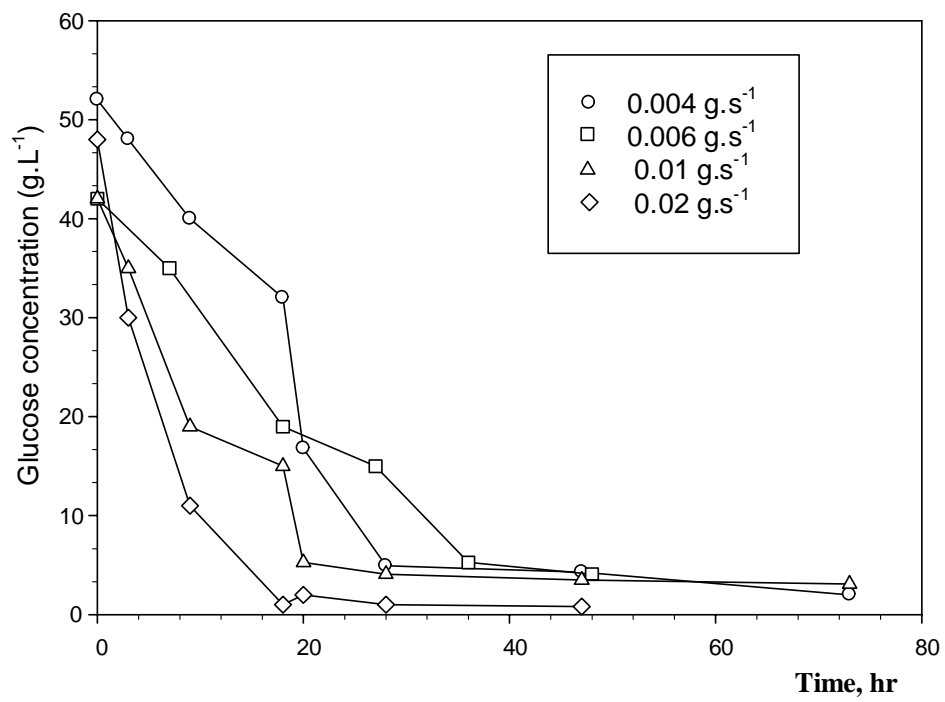


Figure 36 Time course glucose concentration at molasses feeding rate 0.004, 0.006, 0.01 and 0.02 g.s⁻¹.

APPENDIX D

Time course of glucose concentration at initial cell concentrations

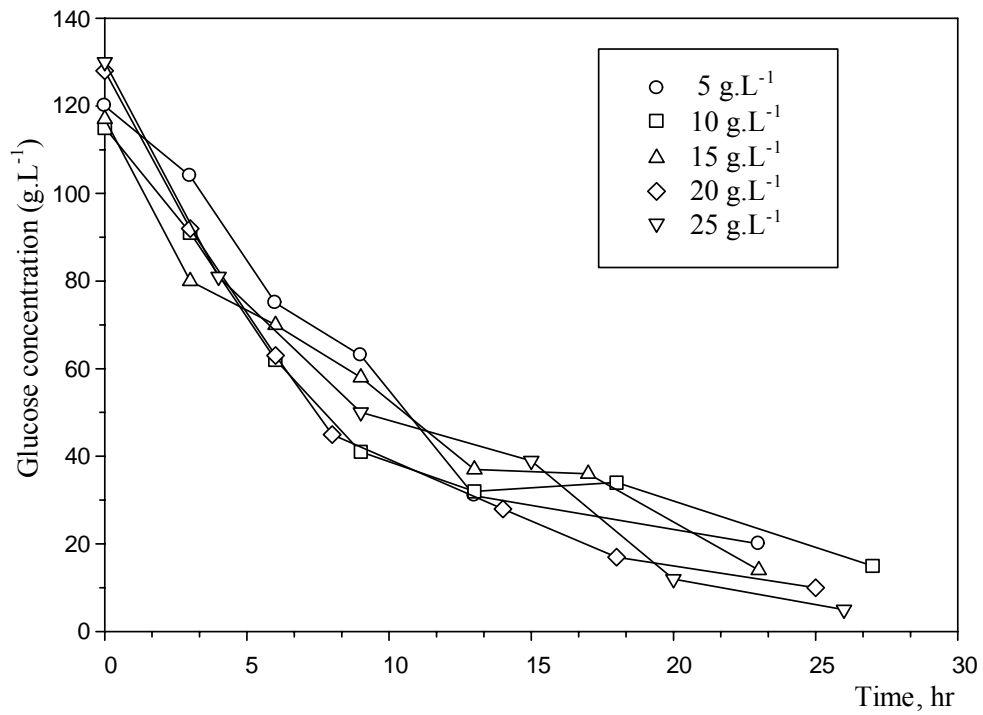


Figure 37 Time course glucose concentration at initial cell concentration 5, 10, 15, 20 and 25 g.L⁻¹

APPENDIX E

Ethanol analysis by gas chromatography

Ethanol analysis by gas chromatography

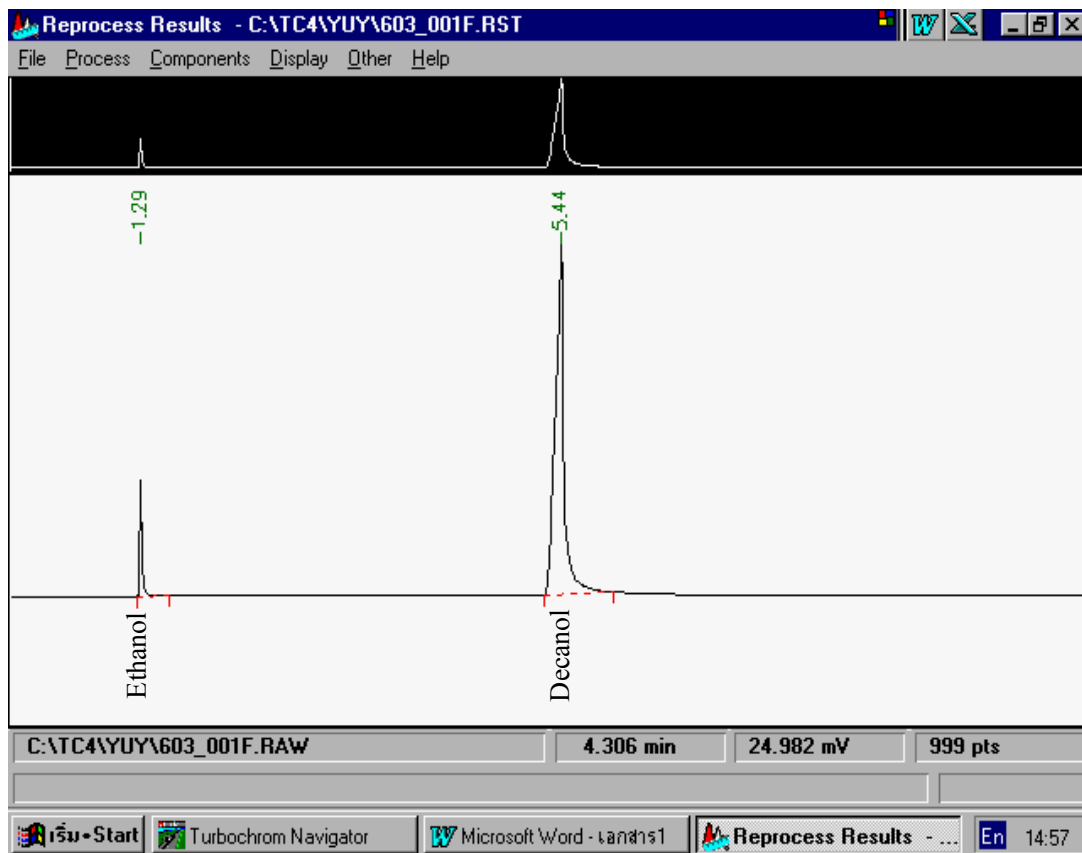


Figure 38 Chromatogram of ethanol and decanol in ethanol extraction from fermentation broths by using perstraction system

Subject presentation: Mass transfer characteristic of ethanol from diluted aqueous solution through silicone membranes in a liquid-liquid contacting system

In

MEMBRANE SCIENCE&TECHNOLOGY 2006 CONFERENCE at Nanyang Technological University, Singapore in 27-28 April 2006 (presentation on 27 April 2006 9.00 - 10.30 am by Oral presentation and poster presentation)

Abstract

Mass transfer characteristic of ethanol from diluted aqueous solution through silicone membranes in a liquid-liquid contacting system

P. Panvichit, S. Kanchanatawee and A. Boontawan*

School of Biotechnology, Institute of Agricultural Technology, Suranaree University of Technology, Nakhon Ratchasima, Thailand 30000.

Abstract

In ethanol fermentation, product inhibition is a major problem affecting both yield and volumetric productivity. This work focused on extraction of ethanol from diluted aqueous solution to organic solvent using dense and composite flat-sheet silicone membranes held in a stainless steel module. Preparation of dense polydimethylsiloxane (PDMS) membranes were carried out using solvent casting technique, whilst composite PDMS membrane supported by polyvinylidene fluoride (PVDF) was fabricated by dry-wet phase inversion method. The experiments were investigated with the membrane thicknesses between 300 to 2 microns. Organic/aqueous (P_{aq}^{org}) and membrane/aqueous (P_{aq}^{mem}) partition coefficients were firstly measured, and were subsequently used to quantify the overall mass transfer coefficients (k_{ov}). Since the membrane had no pore, the problem associated with phase breakthrough could be simply avoided by positive

pressure of the aqueous phase. Effect of operating condition including aqueous, organic Reynolds number, and membrane thickness on the separation performances were investigated. Extraction kinetics were successfully described using a resistance-in-series model, and were controlled by the aqueous boundary layer and membrane resistance (k_{mem}) whilst organic film resistance played an insignificant role to the k_{ov} . Values of k_{ov} were obtained in the range of 3.0×10^{-7} to $4.21 \times 10^{-6} \text{ m.s}^{-1}$. Experimental data showed that increasing of the aqueous hydrodynamic resulted in the increasing of k_{ov} , whereas the values were inversely proportional to the membrane thicknesses.

Keywords: Composite membrane, Mass transfer, Ethanol, Perstraction

* Corresponding author: Tel +66 44 224234; fax +66 44 224154

E-mail address: apichat@sut.ac.th

BIOGRAPHY

Personnel Details: Pailin Panvichit
Date of Birth: 29 December 1982
Martital Status: Single
Nationality: Thai
Home Address: 799 M.11 Sungnoen District, Nakhonratchasima 30170, Thailand
Tel. 0-4441-9755
E-mail Address: panvichit@yahoo.com.

Education:

1994-2000 High school at Sungnoen school, Nakhonratchasima, Thailand
2000-2004 B.Sc. in School of Biotechnology, Mahasarakham University,
Mahasarakham, Thailand.
2004-2006 M.Sc. in School of Biotechnology, Suranaree University of
Technology, Thailand.

Publication:

1. Panvichit, P., Kanchanatawee, S. and Boontawan, A.(2006). **Application of composite PDMS/PVDF membrane in perstraction system of ethanol in fed-batch process from sugar cane molasses (In Thai)**. The first Kaset-Suranaree'49, January 11-15, 2006, Technopolis, Suaranaree University of Technology, Thailand (The oral presentation and poster presentation).
2. Panvichit, P., Kanchanatawee, S. and Boontawan, A.(2006). **Mass transfer characteristic of ethanol from diluted aqueous solution through silicone membranes in a liquid-liquid contacting system**. MEMBRANE SCIENCE & TECHNOLOGY 2006, April 26-29, 2006, Nanyang Technological University, Singapore (Poster presentation).